https://doi.org/10.5194/egusphere-2022-1111
Preprint. Discussion started: 7 November 2022

A plant carbon-nitrogen interface coupling framework in a coupled biophysical-ecosystem-biogeochemical model, SSiB version5/ TRIFFID/DayCent-SOM : Its parameterization, implementation, and evaluation

Zheng Xiang[1,2], Yongkang Xue[2*], Weidong Guo[1,4*], Melannie D. Hartman[3], Ye Liu[2,5], William J. Parton[3]

[1]School of Atmospheric Sciences, Nanjing University, Nanjing, China
[2]Department of Geography, University of California, Los Angeles, CA 90095, USA
[3]Natural Resource Ecology Laboratory, Colorado State University, CO 80523, USA
[4]Joint International Research Laboratory of Atmospheric and Earth System Sciences, Nanjing, China
[5]Pacific Northwest National Laboratory, Richland, WA 99352, USA.

Correspondence to: Yongkang Xue (yxue@geog.ucla.edu), Weidong Guo (guowd@nju.edu.cn)

Abstract. Plant and microbial nitrogen (N) dynamics and N availability regulate the photosynthetic capacity and capture, allocation, and turnover of carbon (C) in terrestrial ecosystems. Studies have shown that a wide divergence in representations of N dynamics in terrestrial surface processes leads to large uncertainty in climate simulations and the projections of future trajectories. In this study, a plant C-N interface coupling framework was developed and implemented in a coupled biophysical-ecosystem-biogeochemical model (SSiB5/TRIFFID/DayCent-SOM). The main concept and structure of this plant C-N framework and its coupling methodology are presented. Different from many current approaches, this framework not only involves soil organic matter cycling, but uniquely takes into account plant N metabolism first, such as plant resistance and self-adjustment, which are represented by dynamic C/N ratios for each plant functional type (PFT). Then, when available N is less than plant N demand, N restricts plant growth, reducing gross primary productivity (GPP), and modulating plant respiration rates and phenology. All these considerations ensure a full incorporation of N regulations to plant growth and C cycling. This new approach has been tested to assess the effects of this coupling framework and N limitation on the terrestrial carbon cycle. Measurements from flux tower sites with different PFTs from 1996-2013 and global satellite-derived observations from 1948-2007 are used as references to assess the effect of the C-N coupling process on the long-term mean vegetation distribution and terrestrial C cycling using the offline SSiB5/TRIFFID/DayCent-SOM model, which use observed meteorological forcing to drive the model. The sensitivity of the terrestrial C cycle to different components in the framework is also assessed. The results show a general improvement with the new plant C-N coupling framework, with more consistent

https://doi.org/10.5194/egusphere-2022-1111
Preprint. Discussion started: 7 November 2022

emergent properties, such as GPP, leaf area index (LAI), and respiration, compared to observations. The main improvements occur in tropical Africa and boreal regions, accompanied by a decrease of the bias in global GPP and LAI by 16.3% and 27.1%, respectively.

1 Introduction

Land surface processes substantially affect climate (Foley et al., 1998; Ma et al., 2013; Sellers et al., 1986; Xue et al., 2004, 2010) and are influenced by climate in turn (Bonan, 2008; Liu et al., 2019, 2020; Zhang et al., 2015), forming complex feedback loops to climate change (Friedlingstein et al., 2006; Gregory et al., 2009). To study these processes, the land surface components of Earth System Models (ESMs) have evolved from those that only represent biophysical processes (i.e., hydrology and energy cycle) to those that include terrestrial carbon (C) cycle, vegetation dynamics, and nutrient processes (Cox et al., 2001; Dan et al., 2020; Foley et al., 1998; Jiang et al., 2014; Lu et al., 2001; Niu et al., 2020; Oleson et al., 2013; Pan et al., 2017; Sellers et al., 1986; Sitch et al., 2003; Wang et al., 2010a; Yang et al., 2019). Current land surface models have large uncertainties in predicting historical and recent C exchanges (Beer et al., 2010; Richardson et al., 2012; Zaehle et al., 2015), and have been criticized for being oversimplified from an ecological point of view (Reich et al., 2006) and for overestimating terrestrial C sequestration (Hungate et al., 2003; Thornton et al., 2007). The uncertainty/errors in predictions using land models have been attributed to many factors, with inclusion or exclusion of nutrient limitations as one of the critical factors. Those C-only models ignore significant nitrogen (N) impacts. As such, C sequestration by terrestrial ecosystems under climate change is overestimated (Peñuelas et al., 2013; Zaehle et al., 2015). Ecosystem N cycling processes are among the dominant drivers of terrestrial C-climate interactions, which affect vegetation growth and productivity (Reich et al., 2006), especially in N-poor younger soils at high latitudes (LeBauer & Treseder, 2008; Vitousek and Howarth, 1991) mainly through N limitation, as well as microbial decomposition of organic matter (Hu et al., 2001). Therefore, the N cycle and its effect on C uptake in the terrestrial biosphere has been incorporated in land surface models (LSMs) of ESMs (Davies-Barnard et al., 2020) with various representations of N processes (Ali et al., 2015; Best et al., 2011; Clark et al., 2011; Ghimire et al., 2016; Goll et al., 2017; Krinner et al., 2005; Matson et al., 2002; Oleson et al., 2013; Thum et al., 2019; Wang et al., 2010; Yu et al., 2020; Zhu et al., 2019). Despite recent progress, coupling of N processes is still an area of model development. In the latest CMIP6 (Eyring et al., 2016), although there were 112 different coupled models with various land surface models from 33 research teams, only about 10 models incorporated an N cycle module (Arora et al., 2020) with various deficiencies. Among these models including N processes, most of them still focus on microbial N dynamics in soil. The consideration of C-N coupling in plant N processes is not sufficient (Ghimire et al., 2016; Goll et al., 2017; Thum et al., 2019; Yu et al., 2020; Zaehle et al., 2015; Zhu et al., 2019). Although a few key plant N processes, such as N limitation on GPP, the effect of biomass N content on autotrophic respiration, plant N uptake, ecosystem N loss and biological N fixation, have been introduced into LSMs; usually only one or two components are selected with various complexity to present the N limitation effects in current land models. They include, for instance, using N to scale down the photosynthesis parameter $V_{c,max}$ (Ghimire et al., 2016;

https://doi.org/10.5194/egusphere-2022-1111
Preprint. Discussion started: 7 November 2022

Zaehle et al., 2015) or potential GPP to reflect N availability (Gerber et al., 2010; Oleson et al., 2013; Wang et al., 2010a); defining a "C cost of N uptake" (Fisher et al., 2010); and optimizing "N allocation for leaf processes" (Ali et al., 2015). In many of these approaches, N limitation is represented as instantaneous down-regulation of potential photosynthesis rates based on soil mineral N availability.

This paper presents our recently developed process-based approach, which mainly focuses on the plant resistance and N limitation effects on photosynthesis, plant respiration, and plant phenology. The plant C/N ratio is a key concept in representing plant resistance, self-adjustment, and C/N interactions. Due to their relative immobility, plants often face significant challenges in obtaining an adequate supply of nutrients to meet the demands of basic cellular processes. A deficiency of any type of nutrient may result in decreased plant productivity and/or fertility (McDowell et al., 2008; Morgan and Connolly, 2013; Stenberg and Muola, 2017). As such, the plant C/N ratios have to change over the plant's lifecycle with nutrient availability (Meyer-Grünefeldt et al., 2015) through plant self-adjustment. Plant C/N ratios are influenced by the accumulation of C polymers such as carbohydrates and lipids, and are greatest when cells are nutrient starved, or exposed to high light (Aber et al., 2003; MacDonald et al., 2002; Talmy et al., 2014). However, many land models specify fixed plant C/N ratios for each plant functional type (PFT) (e.g., Best et al., 2011; Clark et al., 2011; Krinner et al., 2005; Oleson et al., 2013; Wang et al., 2010b). In this paper, we present a new plant C-N coupling framework with flexible C/N ratios (Section 4.2), in which N regulates photosynthesis (Section 4.3), respiration (Section 4.4), and plant phenology (Section 4.5), as well as produces a consistent coupling between biophysical and biogeochemical processes. Allometric relations and empirical data sets are used to constrain the range of possible C/N ratios. This dynamic C/N ratio depends on the degree which the N demands of different plant organs (e.g., leaf, root, and wood) are satisfied over the past several days. This plant C-N framework can simulate the plant N metabolism and prevent unrealistic instantaneous down-regulation of potential photosynthesis rates.

We implement this plant C-N framework by coupling a soil organic matter and nutrient cycling model (DayCent-SOM) with a biophysical/dynamic vegetation model (SSiB5/TRIFFID, the Simplified Simple Biosphere Model version 5/ Top-down Representation of Interactive Foliage and Flora Including Dynamics Model, Cox, 2001; Harper et al., 2016; Liu et al., 2019; Xue et al., 1991; Zhan et al., 2003; Zhang et al., 2015). DayCent-SOM, which includes only the soil organic matter (SOM) cycling and trace gas subroutines from the DayCent ecosystem model (Parton et al., 1998; 2010) represents SOM transformations, below-ground N cycling, soil N limitation to microbial processes and plant growth, and nitrification/denitrification processes. In the coupled model, the potential N uptake depends on plant N demand from a biophysical and dynamic vegetation model, SSiB5/TRIFFID. The actual plant N uptake is limited based on soil N availability as predicted by DayCent-SOM (Del Grosso et al., 2000; Parton et al., 1998; 2010). The coupled model is verified at twelve flux tower sites with different PFTs and is used to conduct several sets of global 2-D offline simulations from 1948 to 2007 to assess the effects of the coupling process. The model predictions of global GPP and LAI are evaluated against satellite-derived observational data. The results demonstrate the relative importance of different plant N processes in this C-N framework.

The model and data used in this paper are presented in section 2. In section 3, the experimental design is described. The development and implementation of this plant C-N framework is presented in Section 4. In section 5, the measurements from

https://doi.org/10.5194/egusphere-2022-1111
Preprint. Discussion started: 7 November 2022

the flux tower sites with different PFTs and the global satellite-derived observations from 1948-2007 are used as references to assess the effect of the C-N coupling process on the long-term mean vegetation distribution and terrestrial C cycling using the offline the SSiB5/TRIFFID/DayCent-SOM. Some issues and conclusions are presented in section 6.

2 Models and Data

2.1 SSiB4/TRIFFID model

The Simplified Simple Biosphere Model (SSiB, Xue et al., 1991; Sun and Xue, 2001; Zhan et al., 2003) is a biophysical model that simulates soil moisture and temperature, runoff, fluxes of sensible/latent heat, surface radiation and momentum, and vegetation GPP based on water and energy balances and photosynthesis processes. A dynamic vegetation model, the Top-down Representation of Interactive Foliage and Flora Including Dynamics Model (TRIFFID) is employed by SSiB to calculate NPP, LAI, canopy height, and PFT fractional coverage according to the C balance (Cox, 2001; Harper et al., 2016; Liu et al., 2019; Zhang et al., 2015). Moreover, the surface albedo and aerodynamics resistances are also updated based on the vegetation conditions. Zhang et al. (2015) had improved plant physiology processes and the PFT competition strategy to make the SSiB4/TRIFFID suitable for seasonal, interannual, and decadal studies. Seven PFTs are included: (1) broadleaf evergreen trees (BET), (2) needleleaf evergreen trees (NET), (3) broadleaf deciduous trees (BDT), (4) C3 grasses, (5) C4 plants, (6) shrubs, and (7) tundra. PFT coverage is determined by net C availability, competition between species, and disturbance, which includes mortality due to fires, pests, and windthrow. A detailed description and validation of SSiB4/TRIFFID can be found in Zhang et al., (2015), Liu et al., (2019), and Huang et al. (2020). In this study, The DayCent-SOM (see next section) is introduced and coupled with the SSiB5/TRIFFID using the C-N interface coupling framework introduced in this study, which will be discussed in Section 4.

2.2 DayCent-SOM model

DayCent is a daily version of the CENTURY ecosystem model (Parton et al., 1998; Del Grosso et al., 2000), which is widely used to simulate major processes associated with C, N, phosphorus (P), and sulfur (S) cycling in a plant-soil system. The model also simulates agriculture land management practices.. Several key processes are included, such as decomposition of litter and soil organic matter (SOM); mineralization/immobilization and plant uptake of nutrients; N-gas emissions from nitrification and denitrification; and CH_4 oxidation in non-saturated soils (i.e., methanotrophy). Litter and SOM decomposition is controlled by soil moisture, temperature, pH, and tillage intensity. Model inputs are daily weather data (e.g., maximum and minimum air temperature, solar radiation, precipitation, relative humidity, and wind speed), soil properties, and land management and disturbance data (e.g., fire, biomass harvest, flooding, and storm damage).The DayCent model has been used to simulate NPP, soil organic C, N_2O emissions, nitrate leaching, and CH_4 oxidation in natural and managed systems with extensive validations (Del Grosso et al., 2000, 2005; Parton et al., 2010). DayCent-SOM, a subset of DayCent that excludes the larger model's plant growth, soil hydrology, and soil temperature subroutines, consists of soil mineral N pools (ammonium and nitrate) and five

https://doi.org/10.5194/egusphere-2022-1111
Preprint. Discussion started: 7 November 2022

types of organic C and N pools consisting of two plant litter pools (metabolic and structural) and three kinetically defined organic matter pools, (active, slow, and passive); all organic pools except the passive pool have both above-ground and below-ground counterparts. DayCent-SOM is forced with soil temperature, soil moisture, soil water flow, and plant C and N litter inputs from SSiB5/TRIFFID, and computes daily changes to all organic matter and mineral soil pools, estimates losses of N from nitrate leaching and N_2O, NO_x, and N_2 emissions, estimates the amount of inorganic N available to plants (N_{avail}), and updates inorganic N pools based on plant N-uptake. The full description for plant N uptake and soil N dynamics is available in Parton et al. (1994, 1998) and Del Grosso et al. (2000).

2.3 The computational flow of SSiB5/TRIFFID/DayCent-SOM

In SSiB5/TRIFFID/DayCent-SOM, GPP, autotrophic respiration, and other physical variables such as canopy temperature and soil moisture are provided by SSiB5 every 3 hours for TRIFFID (Fig. 1). TRIFFID accumulates the GPP and respiration from SSiB5 and predicts biotic C, vegetation height, LAI and PFT fractional coverage, every ten days, which are used to update surface properties, such as albedo, roughness length, and aerodynamic/canopy resistances, in SSiB5. The plant C-N framework uses the meteorological forcings (i.e., air temperature and precipitation) and physical variables (i.e., soil moisture and soil temperature) provided by SSiB5 every 3 hours and the biophysical properties (vegetation fraction and biotic C) provided by TRIFFID, which is updated every ten days. The plant C-N interface framework calculates dynamic C/N ratios, N-limited photosynthesis, N-impacted respiration rate, and N-limited phenology every 3 hours. The C loss and potential N uptake are accumulated within one day in the C-N Interface Framework and plant C and N litter fall are transferred to DayCent-SOM at the end of the day. DayCent-SOM calculates inorganic N available for plant N uptake (N_{avail}) and N losses from nitrate leaching and N-trace gas emissions each day. Using PFT competition strategy, TRIFFID updates the vegetation dynamics based on C balance on Day 10. The updated vegetation dynamics are then sent to SSiB5 as input to reflect the N impact on the C cycle.

https://doi.org/10.5194/egusphere-2022-1111
Preprint. Discussion started: 7 November 2022

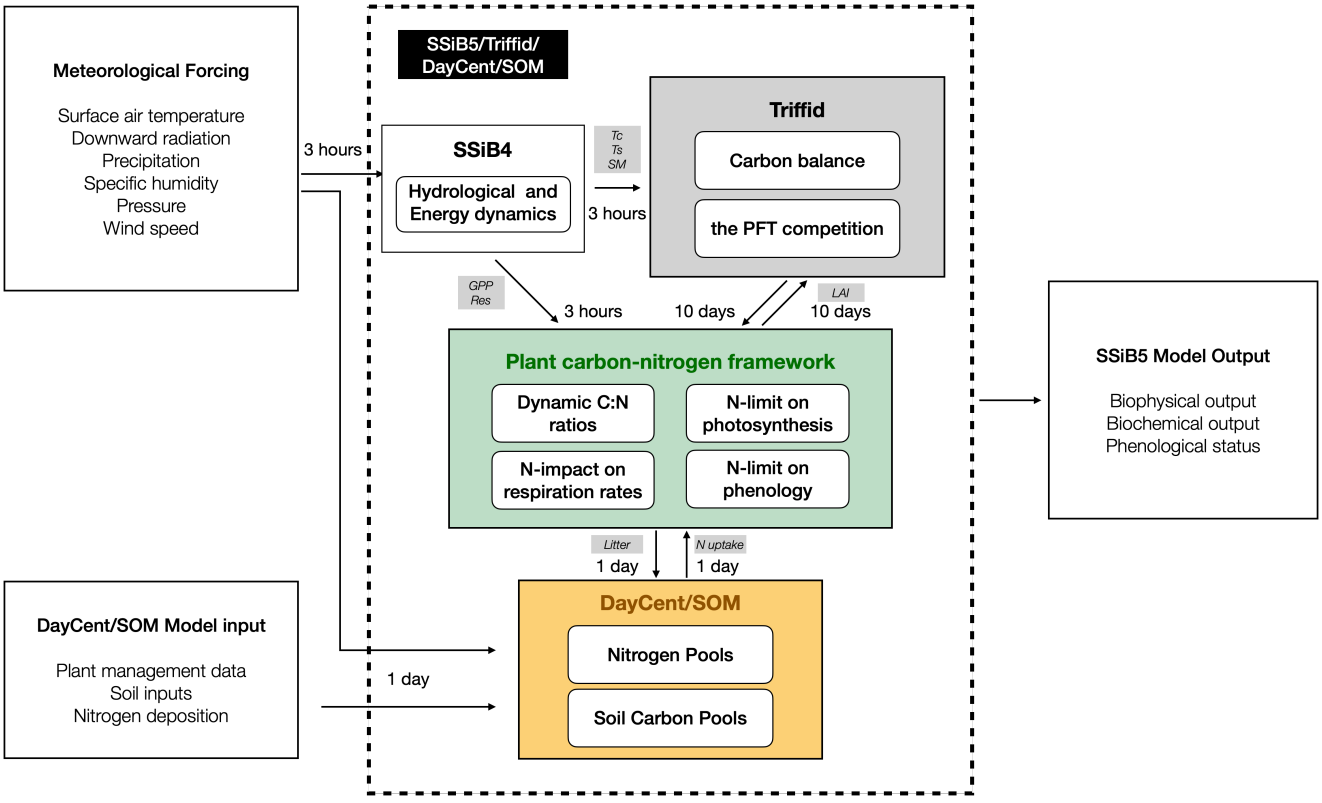

Figure 1. The flowchart of plant carbon-nitrogen interactions in SSiB5/TRIFFID/DayCent-SOM, main variables are listed between two modules.

Notes: Tc: canopy temperature; Ts: land surface temperature; SM: soil moisture; GPP: gross primary productivity; Res: autotrophic respiration.

2.4 Model forcing and validation data

2.4.1 Ground measurement data

To validate the coupled model, twelve sites with representative biome types and climates zones were selected to evaluate the simulations of seasonal patterns of GPP, sensible heat flux and latent heat flux at these sites. The driving data were a half-hourly dataset, including air temperature, specific humidity, wind velocity, air pressure, precipitation, and short- and longwave radiation data from the FLUXNET 2015 dataset (Pastorello et al., 2020). The geographical distribution of selected FLUXNET 2015 sites is displayed in Figure 2 and the detailed site information is listed in Table 1.

https://doi.org/10.5194/egusphere-2022-1111
Preprint. Discussion started: 7 November 2022

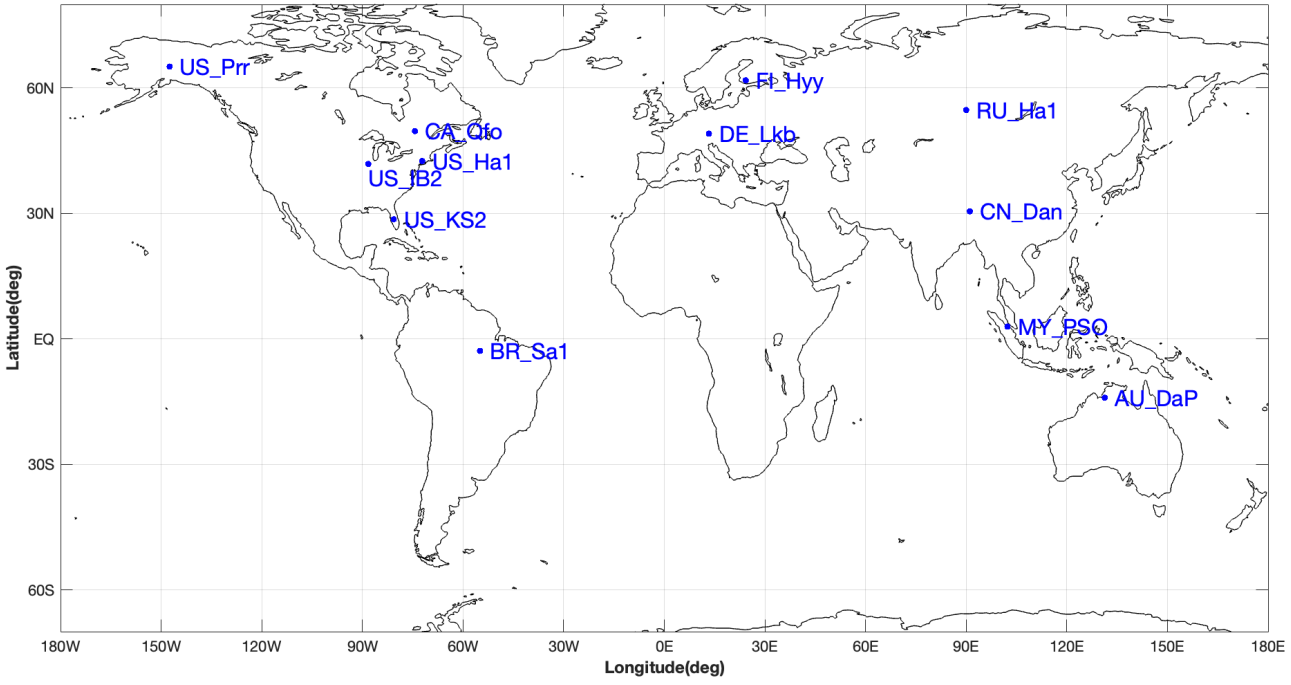

Figure 2. Geographical distribution of selected FLUXNET 2015 sites. The information of these FLUXNET sites is listed in Table 1.

165

Table 1. FLUXNET sites, latitude (LAT), longitude (LONG), plant function type (PFT), and time frame (Time) used for SSiB5/TRIFFID/ DayCent-SOM model validation.

Site_ID	Site name	LAT	LONG	PFT	Time
AU_DaP	Daly River Savanna	-14.06	131.32	C4 grass	2007-2013
BR-Sa1	Santarem-Km67-Primary Forest	-2.86	-54.96	Broadleaf Evergreen	2002-2011
CA_Qfo	Quebec - Eastern Boreal, Mature Black Spruce	49.69	-74.34	Needleleaf Evergreen	2003-2010
CN-Dan	Dangxiong	30.50	91.07	C3 grass	2004-2005
DE_Lkb	Lackenberg	49.10	13.30	Needleleaf Evergreen	2009-2013
FI_Hyy	Hyytiala	61.85	24.29	Needleleaf Evergreen	1996-2014
MY_PSO	Pasoh Forest Reserve	2.97	102.31	Broadleaf Evergreen	2003-2009
RU_Ha1	Hakasia steppe	54.73	90.00	C3 grass	2002-2004
US_Ha1	Harvard Forest EMS Tower (HFR1)	42.54	-72.17	Broadleaf deciduous	1991-2012
US_IB2	Fermi National Accelerator Laboratory- Batavia (Prairie site)	41.84	-88.24	C3 grass	2004-2011
US-KS2	Kennedy Space Center (scrub oak)	28.61	-80.67	Shrub	2003-2006
US_Prr	Poker Flat Research Range Black Spruce Forest	65.12	-147.49	Needleleaf Evergreen	2010-2014

https://doi.org/10.5194/egusphere-2022-1111
Preprint. Discussion started: 7 November 2022

2.4.2 Meteorological forcing data

The Princeton global meteorological dataset for land surface modelling (Sheffield et al., 2006) was constructed by combining a suite of global observation-based datasets with the National Center for Environmental Prediction/National Center for Atmospheric Research reanalysis data. We use this dataset to drive SSiB4/TRIFFID global simulations from 1948 to 2007 at a 3-hour temporal interval with 1° x 1° spatial resolution. This dataset includes surface air temperature, pressure, specific humidity, wind speed, downward short-wave radiation flux, downward long-wave radiation flux, and precipitation.

2.4.3 Global remote-sensing data

Two widely used global LAI products were used as references to assess the climatological status, variation, and trends of simulated LAI in this study: the Global Inventory Modeling and Mapping Studies (GIMMS) LAI and the Global LAnd Surface Satellite (GLASS) LAI. GIMMS-LAI (from 1981 to 2011 with 1/12-degree resolution) is based on the third generation of Normalized Difference Vegetation Index (NDVI3g) from the GIMMS group and an Artificial Neural Network model (Zhu et al., 2013). GLASS-LAI is generated by general regression neural networks from Advanced Very High Resolution Radiometer (AVHRR) (from 1982 to 1999 with 0.05-degree resolution) and MODIS (from 2000 to 2012 with 1 km resolution) reflectance data (Xiao et al., 2014). GIMMS and GLASS LAI were remapped to 1-degree spatial resolution and a monthly temporal interval for overlap period 1982 to 2007.

To evaluate simulated GPP, the Model Tree Ensemble (MTE) GPP product (Jung et al., 2009) was resampled to 1-degree spatial and a monthly temporal resolution and used as the reference. MTE used a machine learning technique in which the model was trained to predict the C fluxes at FLUXNET sites driven by observed meteorological data, land cover data, and the remotely-sensed fraction of absorbed photosynthetic active radiation. , and then was applied at the grid-scale driven by gridded forcing data (Jung et al., 2009). However, the MTE data do not include CO_2 fertilization. Liu et al. (2019) discuss this issue and indicate that the lack of CO_2 fertilization mainly affects the trend. Since this paper focuses on climatological mean as well as differences between different experiments in which the CO_2 fertilization effect would be largely cancelled, the missing CO_2 fertilization in the FLUXNET-MTE is not a factor in interpreting our results.

3 Experimental design

3.1 Initial condition for the dynamic vegetation model

The initial condition of the dynamic vegetation SSiB4/TRIFFID needs to be obtained from a long-term equilibrium simulation (Zhang et al., 2015). There are different ways to initialize the surface condition for the quasi-equilibrium simulation. Following previous SSiB4/TRIFFID studies (Zhang et al., 2015; Liu et al., 2019; Huang et al., 2020), we set up the initial condition for the run using the SSiB vegetation map and SSiB vegetation table, which are based on ground surveys and satellite-derived information (Dorman & Sellers, 1989; Sellet et al., 1996; Xue et al., 2004; Zhang et al., 2015) with 100% occupation at each

https://doi.org/10.5194/egusphere-2022-1111
Preprint. Discussion started: 7 November 2022

grid point for the dominant PFT and zero for other PFTs. We then ran the SSiB4/TRIFFID model with the climate forcing for 100 years to reach equilibrium conditions. The vegetation and soil conditions from the equilibrium results were used as the initial conditions for the subsequent model runs.

Determining the initial conditions for SSiB5/TRIFFIID/DayCent-SOM was carried out as described for SSiB4/TRIFFID with one additional step in order to initialize global soil C and N levels. We saved 60 years of daily litter C/N inputs and soil temperature and moisture conditions from SSiB4/TRIFFID that were based on historical meteorological forcings (1948-2007). An offline version of DayCent-SOM was run for 2000 years for each grid cell using these 60 years of data, repeated over and over, to determine quasi-equilibrium soil C & N levels; these soil C and N values were read in by SSiB5/TRIFFIID/DayCent-SOM at the start of the global simulation in 1948.

3.2 Site-level validation

This paper focuses on the impact of N processes on the climatology of the global carbon cycle. Most current Dynamic Global Vegetation Models (DGVMs) are mainly focused on long-term (decadal to thousands of years or even longer) simulations at global scale; the diurnal and seasonal variations are not a subject for their modelling. Moreover, adequate long term in-situ measurements are also not available for comparison. However, since the SSiB5/TRIFFID is a process-based model, we can take this advantage to evaluate the model's short-term performance using in-situ measurements.

Twelve sites with representative biome types and climates zones (Table 1 and Fig. 2) were selected to evaluate the simulations of seasonal patterns of fluxes over these sites. The site-level simulations were conducted by SSiB4/TRIFFID (a C-only model) and SSiB5/TRIFFID/DayCent-SOM separately to validate the model's performance. The observed vegetation situations were used as the initial conditions. The model results were compared against observed daily data obtained by the flux tower including GPP, sensible heat flux, and latent heat flux.

3.3 Global 2-D offline control run and sensitivity runs

In this study, the SSiB4/TRIFFID and the SSiB5/TRIFFID/DayCent-SOM were applied to conduct a series of global 2-D offline runs (Table 2). All these runs employed the quasi-equilibrium simulation results as the initial condition, then were driven by the historical meteorological forcing from 1948 through 2007. The run using the SSiB4/TRIFFID is referred to as the control run (Exp. SSiB4 hereafter). Using the control simulation, we first evaluated the ability of the model to produce the climatology and variability of several biotic variables by comparing it to multiple observation-based datasets. In addition to the control run, four sets of sensitivity experiments were conducted to quantify the major effects of the N process and C-N interface coupling methodology on the C cycle. These sensitivity experiments were designed as follows:

(1) Nitrogen limitation on photosynthesis (Exp. NlPSN): The same meteorological forcing used for the control (Exp. SSiB4) drives the model, but dynamic C/N ratios and N limitation on $V_{c,max}$ (Eq. 7) are introduced. The difference between Exp. SSiB4 and Exp. NlPSN indicates the effect of N limitation on photosynthesis.

https://doi.org/10.5194/egusphere-2022-1111
Preprint. Discussion started: 7 November 2022

(2) Nitrogen limitation on NPP (Exp. NlNPP): The same meteorological forcing used for the control (Exp. SSiB4) drives the model, but dynamic C/N ratios and N limitation on NPP are introduced (Eq. 9a). The difference between Exp. SSiB4 and Exp. NlNPP indicates the effect of N limitation on NPP.

(3) Nitrogen limitation on GPP (Exp. NlGPP): The same meteorological forcing used for the control (Exp. SSiB4) drives the model, but dynamic C/N ratios and N limitation on GPP are introduced (Eq. 9b). The difference between Exp. SSiB4 and Exp. NlGPP indicates the effect of N limitation on GPP. Please note, the limitation in 1st sensitivity experimental is applied to $V_{c,max}$, i.e., during the process of photosynthesis computation; while the 3rd sensitivity experiment is applied to the limitation to GPP, i.e., the final photosynthesis products.

The above three approaches have been commonly used in recent C-N coupling for the N limitation as discussed in Introduction (Ghimire et al., 2016; Zaehle et al., 2015; Gerber et al., 2010; Oleson et al., 2013; Wang et al., 2010). The comparison of these three sets of experiments will indicate the uncertainty caused by these three different approaches.

(4) SSiB5/TRIFFID/DayCent-SOM (Exp. SSiB5): The model was driven by the same meteorological forcing used for Exp. SSiB4, but all four C-N coupling processes in the framework, i.e., dynamic C/N ratio, N impacts on photosynthesis, autotrophic respiration, and phenology, are introduced. The difference between Exp. SSiB4 and Exp. SSiB5 indicates the effect of N dynamics, especially the sensitivity of C cycle variability and trend to N process coupling. Furthermore, the difference between Exp.NlPSN and Exp. SSiB5 indicates the uncertainty (or possible errors) due to missing N effect on autotrophic respiration and phenology in the coupling framework.

Table 2. Experimental design

100-year equilibrium	*Initial condition* →	Real-forcing simulation 1948-2007
Fixed climatology forcing		*Transient forcing*
Control experiment		**SSiB4:** Control experiment **NlPSN:** **N**itrogen **l**imitation on **p**hotos**y**n**t**hesis(Vmax) **NlNPP:** **N**itrogen **l**imitation on photosynthesis(**NPP**) **NlGPP:** **N**itrogen **l**imitation on photosynthesis(**GPP**) **SSiB5:** including all four nitrogen processes

4 The Development of a plant Carbon-Nitrogen (C-N) Interface coupling framework

4.1 The conceptual considerations and coupling strategy

To represent C/N interactions, we have developed a plant C-N interface framework to take into account both biophysical and biochemical C/N processes in plant life activities. In this study, we applied the coupling framework to

https://doi.org/10.5194/egusphere-2022-1111
Preprint. Discussion started: 7 November 2022

SSiB5/TRIFFID/DayCent-SOM. However, this approach could be applied to any other models with similar physical/biological principles. The conceptual considerations in developing this framework are presented in this section. For a process-based model, introducing a consistent coupling philosophy between biophysical and biogeochemical processes is necessary. The soil N dynamics model (DayCent-SOM) is directly driven by soil temperature/moisture as well as plant C/N litter inputs into soil. Because the surface water, radiation, and carbon fluxes and plant litter are calculated by SSiB5, we force DayCent-SOM with SSiB5-produced soil temperature, soil moisture, and SSiB5-produced plant litter. DayCent-SOM then computes daily changes of all organic matter and mineral soil pools, estimates losses of N from nitrate leaching and N_2O, NO_x, and N_2 emissions, predicts the amount of inorganic N available to plants, and updates inorganic N pools after accounting for plant N uptake by SSiB5. Following plant N-uptake from DayCent-SOM, our plant C-N interface framework describes N effects on plant physiology from photosynthesis, plant autotrophic respiration, and plant phenology plus a dynamic C/N ratio (Fig. 3). Following such model development philosophy, we more realistically represent the physiological processes of C-N cycling with unique features among current LSMs in C-N coupling.

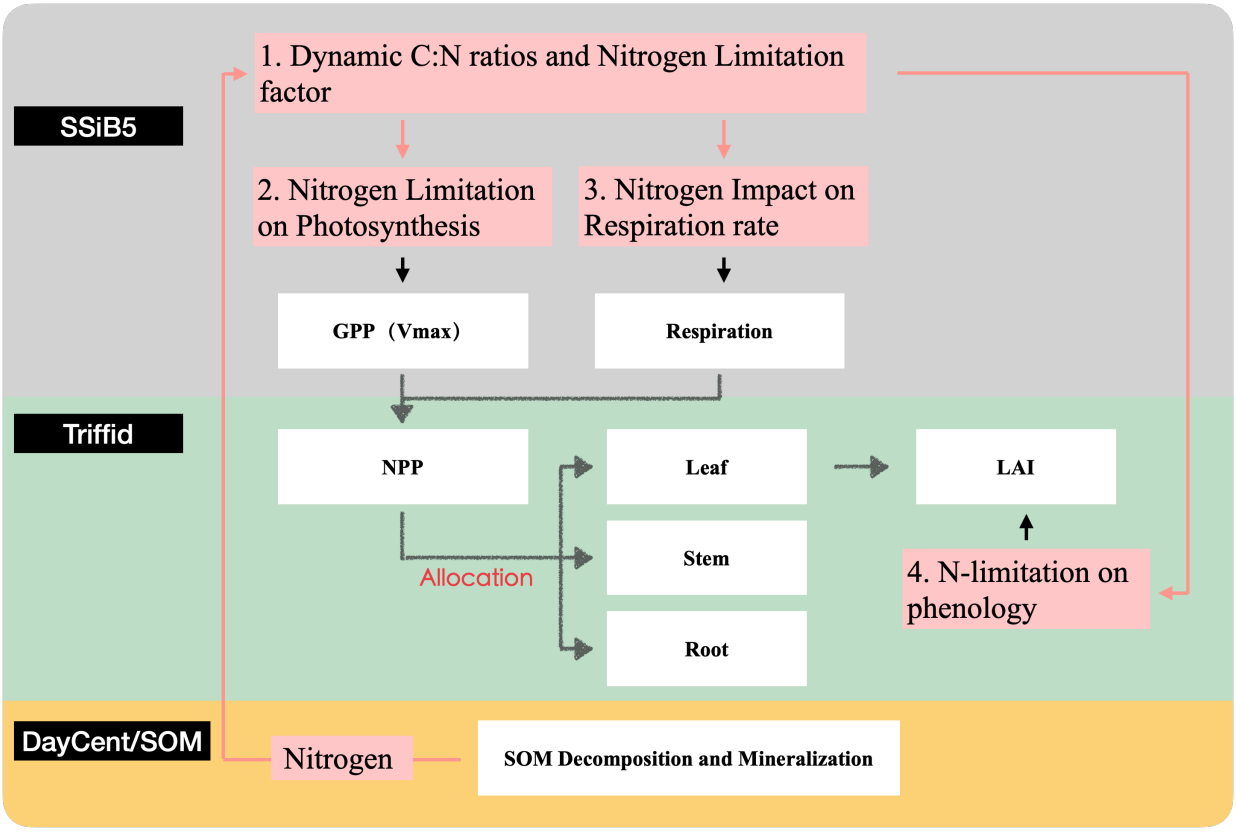

Figure 3. Schematic diagram of plant biogeochemistry and nitrogen impacts in SSiB5/TRIFFID/DayCent-SOM.

https://doi.org/10.5194/egusphere-2022-1111
Preprint. Discussion started: 7 November 2022

Notes: (1) Different background colors represent three different modules: SSiB, TRIFFID, and DayCent/SOM; (2) White boxes indicate the main processes in C-N coupling in different modules; (3) Vermeil boxes indicate how nitrogen influences plant biogeochemistry through our C-N framework.

A commonly used parameterization of photosynthetic C assimilation by the terrestrial biosphere in ESMs is represented by the Farquhar, von Caemmerer, and Berry (FvCB) model of photosynthesis (Collatz et al., 1991; Farquhar et al., 1980). Plants require N as essential components of photosynthetic proteins involved in light capture, electron transport, and carboxylation (Evans, 1989). Nitrogen is an important constituent of the Rubisco enzyme and mitochondrial enzymes that regulate respiration and adenosine triphosphate (ATP) generation (Makino and Osmond, 1991). One of the most important photosynthetic model parameters, the maximum carboxylation rate by the Rubisco enzyme ($V_{c,max}$) is a key parameter in the FvCB model (Farquhar et al., 1980), and has an extensive range across the models depending on the plant N content (Rogers, 2014). Since N is an important component of the Rubisco enzyme, leaf N content will affect $V_{c,max}$ and thus GPP. The original FvCB model has not explicitly considered the N effect on the photosynthesis; while in a number of LSMs an empirical relationship is applied to relate $V_{c,max}$ to leaf N content N_{leaf} to generate the effect of N on photosynthesis, e.g., ,$V_{c,max} = i_v + s_v \times N_{leaf}$, where the intercept ($i_v$) and slope ($s_v$) are derived for each PFT based on observations (Kattge et al., 2009; Raddatz et al., 2007). Moreover, in some coupling approaches, only the relationship between the root N uptake and GPP/NPP is considered to represent the N limitation on C cycles (Ali et al., 2015; Fisher et al., 2010; Ghimire et al., 2016). However, because NPP is the difference between GPP and autotrophic respiration, adjusting NPP or GPP alone may cause the ratio between NPP and respiration to deviate from reality. Using process-based N limitation factor produced from DayCent-SOM to modify $V_{c,max}$ (See section 4.3) is a more realistic way to produce the N effect on the photosynthesis process.

In the original land surface model (SSiB4/TRIFFID), with assumed unlimited N availability and fixed C/N ratios based on PFT, the assimilated C determined the N contents of leaf, stem, and root, and those influenced autotrophic respiration, which influences GPP, LAI, and NPP. However, plants can adjust their resources and stoichiometric requirements. Changes in N resource availability will result in changes to plant C allocation and partitioning. Studies show plants resorb only about 50% of leaf N on average (Aerts, 1996) to conserve nutrients (Clarkson and Hanson, 1980) and to increase nutrient use efficiency (Herbert & Fownes, 1999; Vitousek, 1982). These processes cause a major internal nutrient flux and changes of C/N ratios to reduce the impact of N limitation (Talhelm et al., 2011; Vicca et al., 2012). In addition, plant responses, such as plant resistance and self-adjustment, will be limited under fixed C/N ratios, which affect plant productivity and litter N content, thus driving changes in the underground biogeochemistry and ultimately C and N uptake and storage (Drewniak and Gonzalez-Meler, 2017). A study on the N deposition effect shows that the increase in foliar N under increased N would improve model responses because it allows adaptations in the stoichiometry of C and N (Medlyn et al., 2015). The main impact will be to decrease C/N ratio in leaves, driving increases in productivity and changes soil and litter N content. A dynamic C/N ratio is employed in our framework to more realistically obtain N states and properly represent the effect of N processes (See section 4.2 for more details).

https://doi.org/10.5194/egusphere-2022-1111
Preprint. Discussion started: 7 November 2022

Nitrogen is not only a dominant regulator of vegetation dynamics, GPP, NPP, and terrestrial C cycles; Reich et al. (2008) demonstrate strong relationships between respiration and N limitation based on observational data from various species. At any normal N concentration, respiration rates are consistently lower on average in leaves than in stems or roots. Therefore, we introduce two parameters for stems and roots, respectively, based on PFT to adjust the respiration rate in section 4.4.

Nitrogen also affects plant phenology and can be remobilized to supply spring bud-break or vegetative shoot extension (Kolb and Evans, 2002; Marmann et al., 1997; Millard, 1994; Neilsen et al., 1997). Nitrogen resorption is found during leaf senescence and growth in evergreens (May and Killingbeck, 1992). Because plants need time to turnover, the plant N processes also have a lag effect on plant phenology (Thomas et al., 2015). Phenology in SSiB4/TRIFFID modulates LAI evolution, including leaf mortality, but it is not directly linked to N. Since different N states and supplements will lead to different lags on phenology, we add N impact on plant phenology by introducing a N limitation parameter, which will be discussed in section 4.5.

4.2 Dynamic C/N ratio based on plant growth and soil nitrogen storage

Plant resistance and self-adjustment are represented by dynamic C/N ratios. The N availability for new growth limits the C assimilation rate through the C/N ratio, i.e., the model simulated NPP should be no more than N_{avail} × C/N ratio of new plant material. In the original TRIFFID parameterization, the C/N ratios for different plant components (leaf, root, and wood) are fixed based on plant functional types (Cox, 2001). Changes in C/N ratios occur over the lifecycle of the plant and vary with nutrient availability were are not captured in the original SSiB4/TRIFFID models. However, a linear relationship between C/N ratio (CNR_{actual}) and N_{avail}, based on DayCent's method of determining variable C:N ratios for plants, is introduced to the SSiB5/TRIFFID/DayCent-SOM for each PFT's components (Fig. 4, Eq. 1).

$$CNR_{actual} = \begin{cases} CNR_{max}, & N_{avail} \le N_{demand,min} \\ \frac{N_{avail}-N_{demand.max}}{N_{demand.min}-N_{demand.max}} \times CNR_{min} + \frac{N_{avail}-N_{demand.min}}{N_{demand.max}-N_{demand.min}} \times CNR_{max} & N_{demand,min} < N_{avail} < N_{demand,max} \\ CNR_{min}, & N_{avail} \ge N_{demand,max} \end{cases} \quad (1)$$

where N_{avail} is the amount of soil mineral nitrogen that was available at the end of the previous day (g N m^{-2}) calculated from DayCent-SOM.

https://doi.org/10.5194/egusphere-2022-1111
Preprint. Discussion started: 7 November 2022

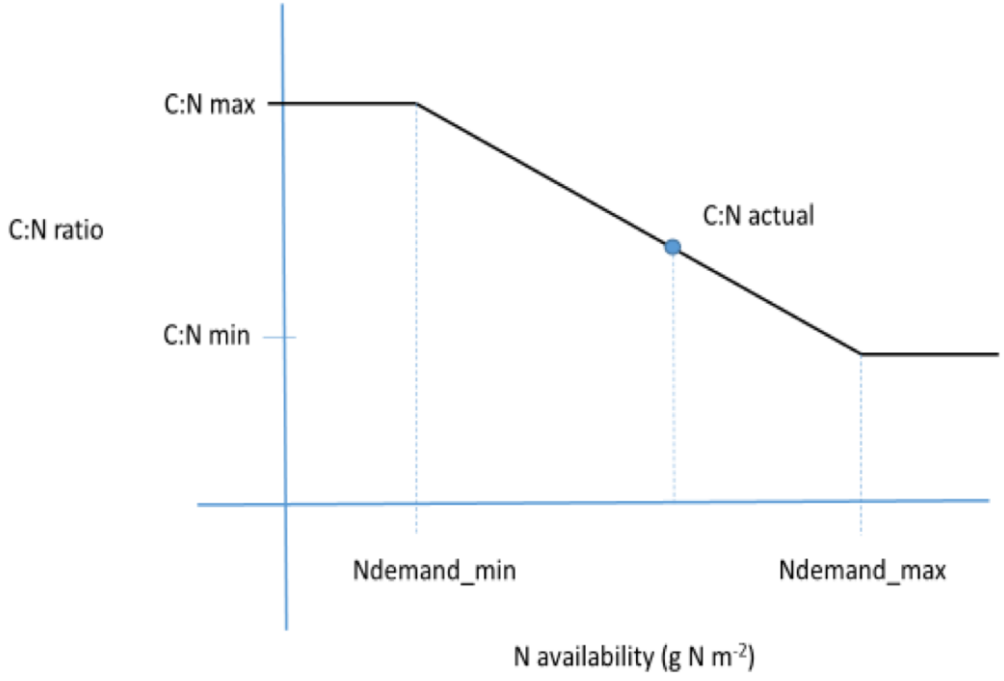

Figure 4. The relationship between the soil nitrogen availability and plant carbon-nitrogen ratios.
Note: CNR_{actual} , CNR_{min}, and CNR_{max} from Eq. 1 are shown as C:N actual, C:N max, and C:N min, respectively, in this figure.

330 The minimum and maximum amounts of nitrogen required ($N_{demand,min}$, $N_{demand,max}$) for the potential NPP_p (g C m^{-2} day^{-1}) that is obtained from SSiB4/TRIFFID are:

$$N_{demand,min} = \frac{NPP_p}{CNR_{max}} \quad (2)$$

$$N_{demand,max} = \frac{NPP_p}{CNR_{min}} \quad (3)$$

where CNR_{min} and CNR_{max} are the minimum and the maximum C/N ratio for each PFT's components (Table 3). The C:N
335 ranges of leaves, fine roots, and stems/wood are from DayCent's user's manual, and other published papers (Parton et al., 1993; Parton et al., 2007). Simulated whole-plant C/N is altered by incremental accumulation of new material with these dynamic C/N ratios.

340

https://doi.org/10.5194/egusphere-2022-1111
Preprint. Discussion started: 7 November 2022

Table 3. C:N ranges of leaves, fine roots, and stems/wood for each plant function type (PFT).

	Plant part	C:N Minimum	C:N Maximum
Broadleaf deciduous	leaves	20	50
	roots	40	70
	wood	200	500
Broadleaf Evergreen	leaves	20	40
	roots	40	70
	wood	150	300
Needleleaf Evergreen	leaves	30	60
	roots	40	60
	wood	400	800
C3 grass	leaves	20	40
	roots	40	50
	wood	40	80
C4 grass	leaves	20	60
	roots	60	100
	wood	60	100
shrub	leaves	20	40
	roots	40	70
	wood	200	400
tundra shrub	leaves	20	40
	roots	40	80
	wood	300	700

Note: CNR_{min} and CNR_{max} from Eq. 1 are shown here as C:N Minimum and C:N Maximum here for each PFT's components. Data are from DayCents user's manual and other publications (Parton et al., 1993; Parton et al., 2007)

Since DayCent-SOM only provides the total available nitrogen ($N_{avail,total}$) for the plant within one grid box, the nitrogen available for each PFT in the grid box and each component for each PFT is calculated as

$$N_{avail} = N_{avail,total} * frac_i * \sum_j Cfrac_{i,j} \quad (4)$$

where $frac_i$ is the fraction of PFT i in one grid, and $Cfrac_{i,j}$ is the fraction of total $N_{avail,total}$ allocated to plant type i, component j, and is determined as

$$Cfrac_{i,j} = \frac{Growth_{i,j}}{\sum_j Growth_{i,j}} \quad (5)$$

where $Growth_{i,j}$ is the amount of new C allocated to plant type i, component j, and is calculated in TRIFFID.

The potential NPP_p that is allocated to each PFT's components is defined similarly as

https://doi.org/10.5194/egusphere-2022-1111
Preprint. Discussion started: 7 November 2022

$$NPP_p = NPP_i * \sum_j Cfrac_{i,j} \quad (6)$$

where NPP_i is the ith type's potential NPP and is calculated in TRIFFID.

4.3 Effect of nitrogen limitation on photosynthesis based on soil available nitrogen and plant C-N ratio

There are several different ways to represent N limitation effects, including using N to scale down photosynthesis (Ghimire et al., 2016; Goll et al., 2017; Thum et al., 2019; Yu et al., 2020; Zaehle et al., 2015; Zhu et al., 2019), using potential gross primary productivity (GPP) to reflect N availability (Gerber et al., 2010; Oleson et al., 2013; Wang et al., 2010), or defining an NPP cost of nitrogen uptake (Fisher et al., 2010). We choose the most physiological way by adjusting $V_{c,max}$ during the photosynthesis process, which regulates both C assimilation and autotrophic respiration, rather than net production (NPP) at the end of the photosynthesis process.

During photosynthesis the assimilation product, GPP, is proportional to the maximum Rubisco carboxylation rate ($V_{c,max}$) which is related to the N concentration.

We therefore introduce a downregulation of the canopy photosynthetic rate based on the available mineral N for new growth (N_{avail}) using a N-availability factor, $f(N)$.

$$V_{c,max-new} = V_{c,max} * f(N) \quad (7)$$

The $f(N)$ is determined by the nitrogen availability:

$$f(N) = \begin{cases} \frac{N_{avail}}{N_{demand,min}} & N_{avail} \le N_{demand,min} \\ 1 & otherwise \end{cases} \quad (8)$$

Plants adjust the relative allocations of C and N during N uptake and via N remobilization and resorption to reduce the impact of N limitation. We assume that there is no N limitation on photosynthesis when $N_{avail} > N_{demand,min}$. We add a linear relationship between $f(N)$ and N_{avail} when N availability is not sufficient for the minimum N demand for new growth. In this approach, a variable ($V_{c,max}$), which is related to N during the photosynthesis process and affects both C uptake and autotrophic respiration, is adjusted.

In fact, the factor, $f(N)$ can also be applied to NPP and GPP as shown in Equations 9a –b and had been done by the studies reviewed at the beginning of this section.

$$NPP_{new} = NPP * f(N) \quad (9a)$$

$$GPP_{new} = GPP * f(N) \quad (9b)$$

If NPP is adjusted (Eq. 9a), this is equivalent to adding a photosynthesis N limitation on plant respiration, which is not reasonable based on plant physiology and may distort the ration of NPP and respiration. In SSiB4/TRIFFID, GPP will be recalculated after determining the potential C achievement. We have designed experiments (Section 3.3) to test all of these approaches and find that they all limit the end production (NPP) of the photosynthesis process, but adjusting $V_{c,max}$ is the most direct and process-based method (See section 5.3 for more discussion).

https://doi.org/10.5194/egusphere-2022-1111
Preprint. Discussion started: 7 November 2022

4.4 Improvement of nitrogen impact on respiration rates based on field observations

Nitrogen affects plant respiration (Reich et al., 2008; Thornely and Johnson, 1990). In the original SSiB4/TRIFFID, the total maintenance respiration (R_{pm}) is given by Cox (2001):

$$R_{pm} = 0.012 R_{dc} \frac{N_l + N_s + N_r}{N_l} \quad (10)$$

where R_{dc} is canopy dark respiration, N_l, N_s and N_r are the N contents of leaf, stem, and root, respectively, and the factor of 0.012 is from the unit conversion. Eq. (10) assumes the respiration rates in root and stem have the same dependence on N content as leaf. However, studies (Reich et al., 2008) have shown that the respiration rates at any common N concentration were consistently lower in leaves than in stems or roots on average.

Thus, we introduce two PFT-specific parameters ($ResA_S$, $ResA_R$) from field observations (Wang et al., 2006; Yang et al., 1992) to represent root and stem respiration.

$$R_{pm} = 0.012 R_{dc} \frac{N_l + ResA_S * N_s + ResA_R * N_r}{N_l} \quad (11)$$

Since $ResA_S$ and $ResA_R$ are generally larger than 1, new R_{pm} is larger than the former one, and the increased respiration due to the nitrogen limitation will decrease the NPP (= GPP – autotrophic respiration). Notably, the R_{dc} calculation linearly depends on $V_{c,max}$ thus the introduced N limitation of $V_{c,max}$ in section 4.3 may also reduce the N effect on respiration.

4.5 N limitation on LAI based on plant phenology

Studies (Aerts and Berendse, 1988; Thomas et al., 2015) show that leaf turnover and aboveground productivity are related to nutrient availability and that plant N processes can potentially lead to lags on phenology. In TRIFFID, a leaf phenology parameter, p, (Cox, 2001) is introduced to represent the vegetation's phenological status, to calculate the leaf drop rate, and to adjust the model-simulated maximum possible LAI, which is based on carbon balance, LAI ($LAI_{balance}$), to actual LAI and produce realistic phenology.

$$LAI = p \times LAI_{balance} \quad (12)$$

and

$$\frac{dp}{dt} = \begin{cases} -\gamma_p & \gamma_{lm} > 2\gamma_0 \\ \gamma_p(1-p) & \gamma_{lm} \le 2\gamma_0 \end{cases} \quad (13)$$

where leaf constant absolute drop rate $\gamma_p = 20\ yr^{-1}$, the leaf mortality rate γ_{lm} is a function of temperature T, and the minimum leaf turnover rate $\gamma_0 = 0.25$ (Cox, 2001). This phenology parameter, p, indicates that "full leaf" is approached asymptotically during the growing season, and p is reduced at a constant absolute rate when the mortality rate is larger than a threshold value. Otherwise, p increases but the rate of increase is reduced as the growing season evolves. To reflect the N limitation in SSiB5/TRIFFID/DayCent-SOM, we assume p, is limited by N availability with the new p determined by

$$p_{new} = f(N) \times p_{original} \quad (14)$$

where $f(N)$ is calculated in section 4.3.

https://doi.org/10.5194/egusphere-2022-1111
Preprint. Discussion started: 7 November 2022

5. Results

5.1 Evaluations using the measurements from twelve sites

In the short-term simulations for 12 sites, both SSiB4 and SSiB5/TRIFFID/DayCent-SOM produce the reasonable seasonal cycle for GPP and surface fluxes (Fig. 5-7, Table 4). The model that includes the C-N coupling framework (SSiB5) in general produces slightly lower absolute bias and root-mean-squared error (RMSE), as well as closer standard deviation for GPP, sensible heat flux, and latent heat flux for the 12 site-averages. However, when comparing SSiB4 to SSiB5 at each site, the simulation closer to observations depends on the flux being evaluated and whether the absolute bias or RMSE is considered. For instance, seven sites show lower absolute bias for GPP with SSiB4 (compared to four sites with SSiB5), but six sites show reduced RMSE for GPP with SSiB5 (compared to four sites with SSiB4). Eight sites show the reduced absolute bias for sensible heat flux with SSiB5 but only five sites show reduced RMSE with SSiB5. Neither SSiB4 nor SSiB5 is consistently negatively or positively biased for GPP and sensible heat flux, but both models tend to be negatively biased for latent heat flux (Fig. 5-7, Table 4). The GPP, sensible heat flux, and latent heat flux averages over 12 sites show slight improvements in both the bias and RMSE with SSiB5. In summary, results indicate that in the short-term simulations with specified initial vegetation conditions, both SSiB4 and SSiB5 produce reasonable GPP and surface heat fluxes compared with in-situ measurements, but adding N processes (SSiB5) shows a slight improvement for the 12-site average.

The tests in this section provide a glance at the model's performance after introducing this C-N coupling framework in several sites with short-term data to gain preliminary confidence. It should be pointed out that SSiB4 and SSiB5 are mainly used for the global studies. For validation of in-situ measurements, proper optimization of some site-specific soil and vegetation parameters are necessary (Xue et al., 1996, 1997). Since this study mainly focuses on the global carbon climatology, the validation for these sites is just to ensure the model is still able to properly represent the surface processes at seasonal scales after introducing the DayCent-SOM through the interface coupling framework; however, no model parameters were optimized during this validation exercise for a better fit between simulated results and FLUXNET measurements. In the following sections a set of long-term experiments are conducted to comprehensively investigate mechanisms governing the global carbon cycle.

https://doi.org/10.5194/egusphere-2022-1111
Preprint. Discussion started: 7 November 2022

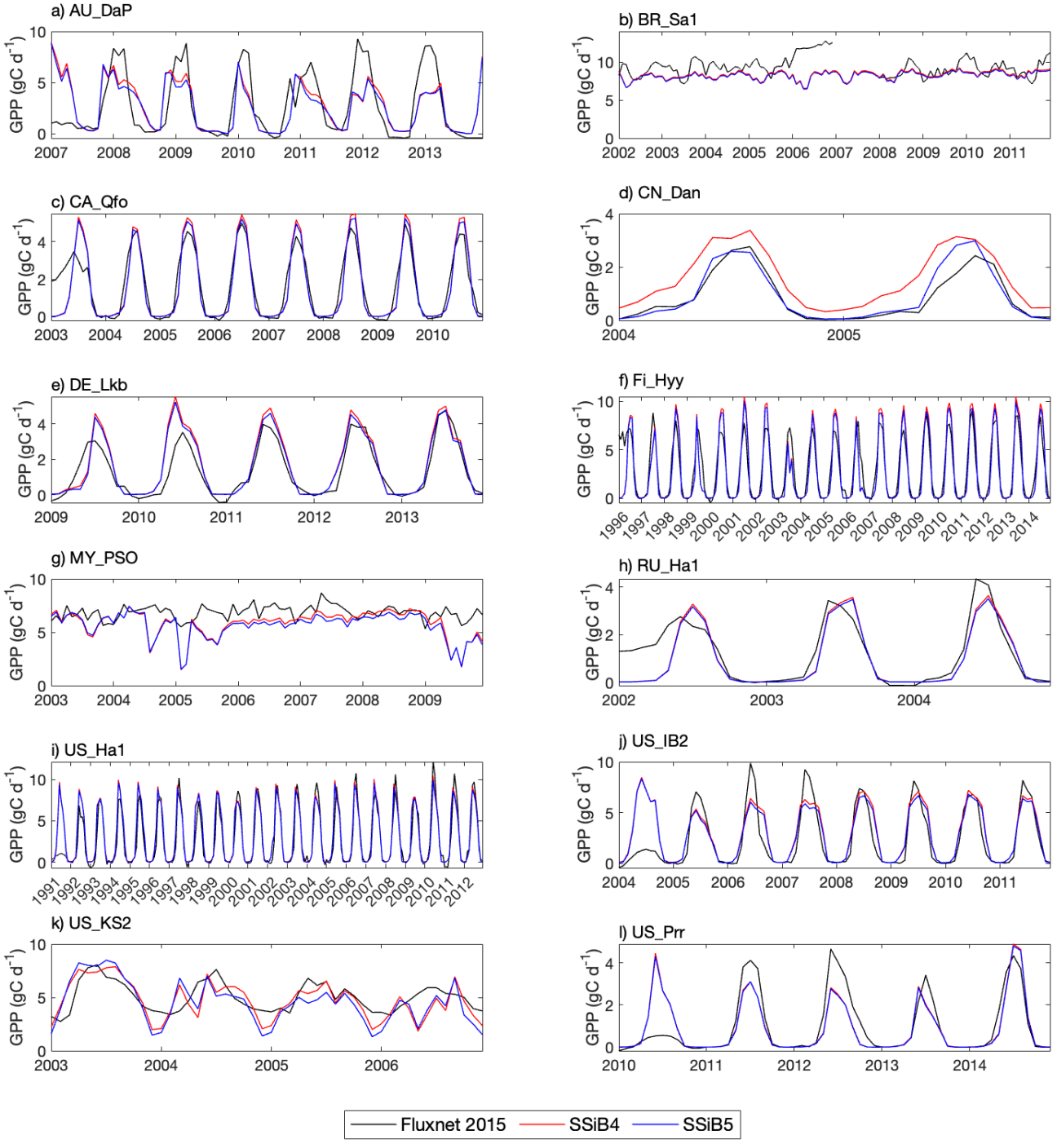

Figure 5. Simulated seasonal variations of GPP against observations at three FLUXNET sites representing different SSiB5 PFTs.
Note: the information of these FLUXNET sites are listed in Table 1.

https://doi.org/10.5194/egusphere-2022-1111
Preprint. Discussion started: 7 November 2022

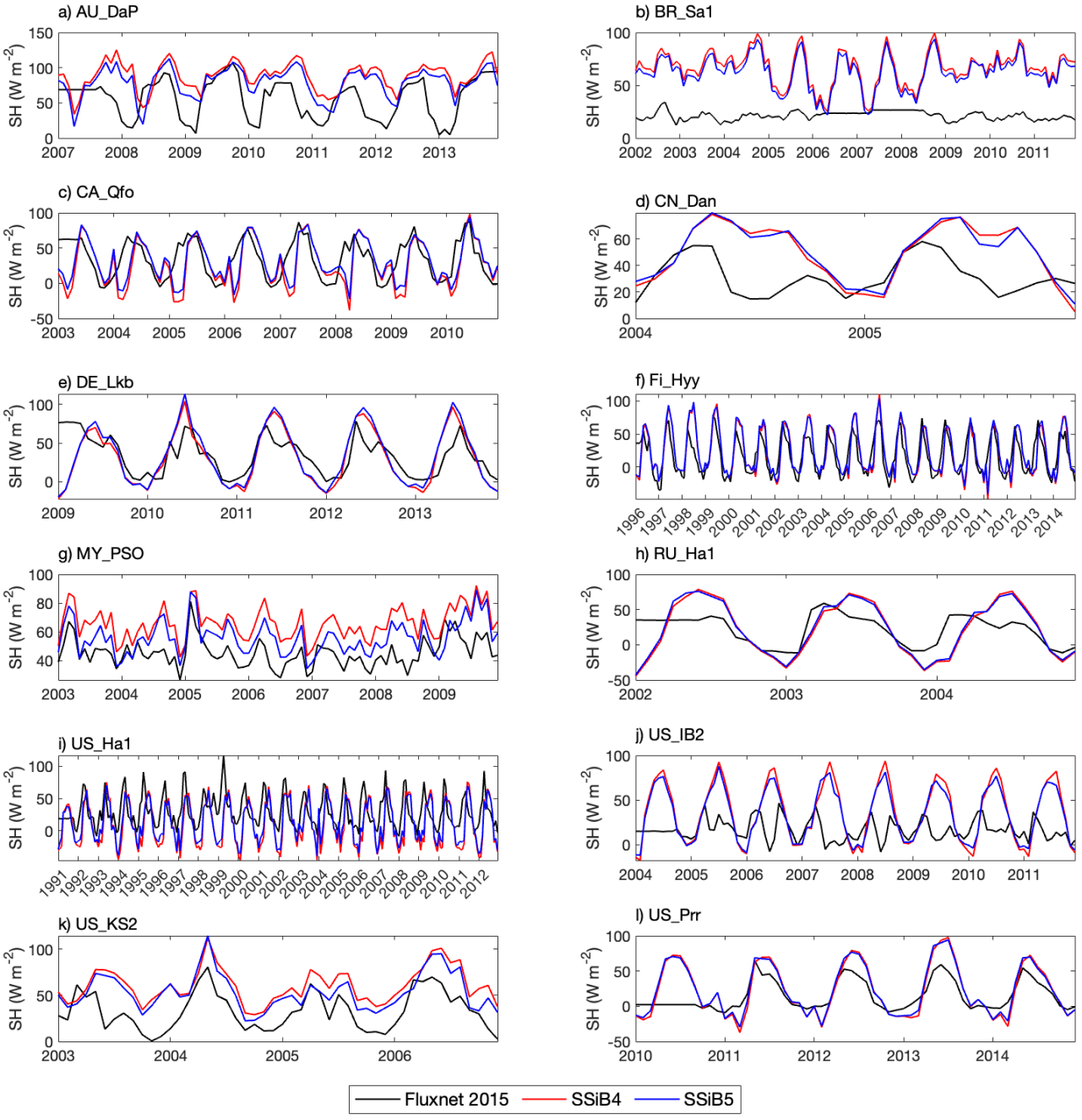

Figure 6. Same as Figure 5, but for sensible heat flux.

https://doi.org/10.5194/egusphere-2022-1111
Preprint. Discussion started: 7 November 2022

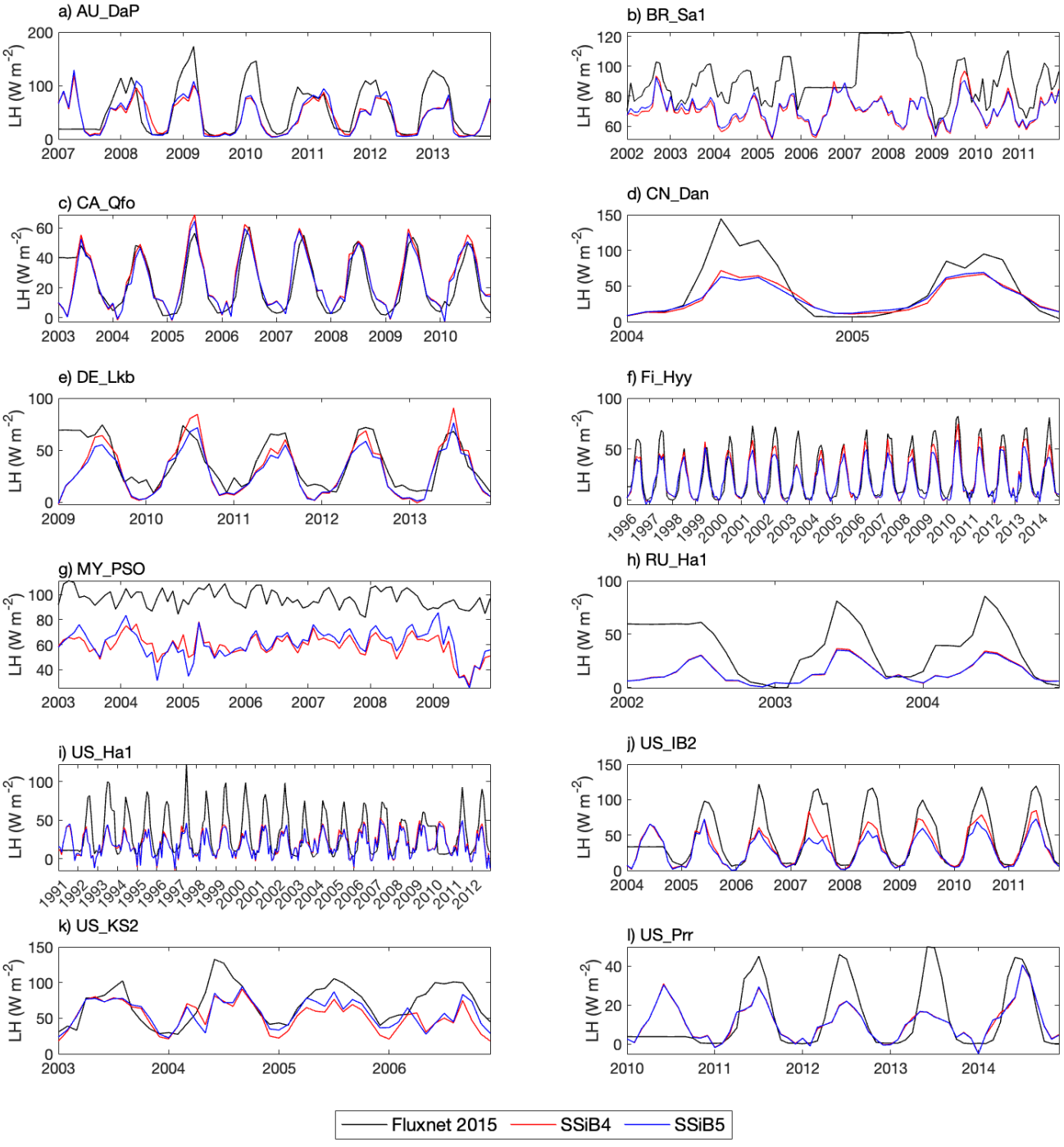

450 **Figure 7.** Same as Figure 5, but for latent heat flux.

https://doi.org/10.5194/egusphere-2022-1111
Preprint. Discussion started: 7 November 2022

Table 4. The GPP, sensible heat flux and latent heat flux intercomparisons of bias, standard deviation and RMSE between SSiB4 and SSiB5 over twelve sites.

	Site_ID	Bias		Standard deviation			RMSE	
		SSiB4	SSiB5	Fluxnet	SSiB4	SSiB5	SSiB4	SSiB5
GPP	AU_DaP	0.05	-0.05	3.11	2.46	2.33	2.60	2.61
(g C d^{-1})	BR-Sa1	-1.07	-1.20	1.31	0.57	0.55	1.77	1.84
	CA_Qfo	-0.05	-0.11	1.71	1.99	1.92	0.78	0.75
	CN-Dan	0.70	0.08	0.92	1.08	1.03	0.80	0.33
	DE_Lkb	0.34	0.25	1.50	1.80	1.71	0.80	0.74
	FI_Hyy	-0.11	-0.22	2.93	3.47	3.32	1.51	1.44
	MY_PSO	-1.02	-1.20	0.65	1.28	1.21	1.63	1.72
	RU_Ha1	-0.24	-0.27	1.29	1.31	1.27	0.69	0.69
	US_Ha1	0.36	0.27	3.31	3.36	3.30	1.31	1.28
	US_IB2	0.56	0.42	2.91	2.70	2.57	1.80	1.79
	US-KS2	-0.28	-0.52	1.37	1.76	2.01	1.35	1.54
	US_Prr	-0.08	-0.10	1.43	1.30	1.28	0.86	0.86
	12-site average	**0.41**	**0.38**	**1.87**	**1.92**	**1.88**	**1.33**	**1.30**
Sensible	AU_DaP	32.47	23.13	28.26	19.64	21.05	36.24	36.32
Heat	BR-Sa1	45.29	40.94	4.04	16.32	15.98	25.61	25.07
Flux	CA_Qfo	-7.04	-2.34	27.77	33.18	29.37	9.54	9.20
(W m^{-2})	CN-Dan	17.96	18.53	14.44	22.38	20.75	25.60	26.99
	DE_Lkb	-3.12	0.16	25.13	35.39	36.91	17.83	18.15
	FI_Hyy	5.53	7.20	28.17	33.57	33.63	8.99	10.91
	MY_PSO	20.49	10.86	10.03	11.30	11.98	39.22	37.99
	RU_Ha1	-0.14	0.84	21.71	39.19	38.02	29.42	29.67
	US_Ha1	-18.34	-15.80	24.40	33.71	29.42	24.33	24.66
	US_IB2	20.21	18.26	11.95	32.89	29.19	23.16	28.72
	US-KS2	27.74	20.81	21.01	19.17	20.14	27.31	24.73
	US_Prr	8.10	9.35	20.93	36.84	35.45	12.02	12.01
	12-site average	**17.20**	**14.02**	**19.82**	**27.80**	**26.82**	**23.27**	**22.70**
Latent	AU_DaP	-11.02	-10.83	45.72	30.03	33.93	36.24	36.32
Heat	BR-Sa1	-20.47	-19.82	16.15	9.44	8.47	25.61	25.07
Flux	CA_Qfo	2.21	0.96	18.06	18.63	17.56	9.54	9.20
(W m^{-2})	CN-Dan	-12.63	-12.57	42.39	22.13	20.77	25.60	26.99
	DE_Lkb	-7.39	-10.00	22.81	24.57	20.79	17.83	18.15
	FI_Hyy	-3.06	-4.84	23.22	19.21	16.64	8.99	10.91
	MY_PSO	-38.18	-36.18	7.07	9.24	11.64	39.22	37.99
	RU_Ha1	-22.89	-23.10	25.68	10.43	10.08	29.42	29.67
	US_Ha1	-11.94	-13.14	27.06	15.53	14.71	24.33	24.66
	US_IB2	-12.90	-17.38	36.91	24.68	20.70	23.16	28.72
	US-KS2	-17.74	-13.41	27.63	20.28	19.65	27.31	24.73
	US_Prr	-1.90	-1.87	16.44	9.62	9.68	12.02	12.01
	12-site average	**13.93**	**13.67**	**25.76**	**17.82**	**17.95**	**24.27**	**23.70**

https://doi.org/10.5194/egusphere-2022-1111
Preprint. Discussion started: 7 November 2022

5.2 Evaluation of GPP and LAI at global scale

The simulated GPP averaged over 1982-2007 is compared to FLUXNET-MTE GPP (Jung et al., 2011) to examine the impact of N processes and its coupling on C and ecosystem characteristics. Both SSiB4/TRIFFID (Exp. SSiB4) and SSiB5/TRIFFID/DayCent-SOM (Exp. SSiB5) capture the distribution of global GPP (Fig. 8). The highest GPP occurs in the tropical evergreen forest and generally decreases with the increase in latitudes in both the observations and the model (Fig. 9). However, Exp. SSiB4's simulated GPP has a negative bias in the Amazon tropical forest and a positive bias in tropical Africa and boreal regions. The simulated global GPP is 1082.36 g C m^{-2} yr^{-1} (Table 5), higher than the estimate, 862.86 g C m^{-2} yr^{-1} in FLUXNET-MTE (Jung et al., 2011). After introducing all N processes, Exp. SSiB5's global GPP prediction, 941.81 g C m^{-2} yr^{-1}, is closer to observations compared to Exp. SSiB4, with a 16.3% reduction in the relative bias (Table 5).

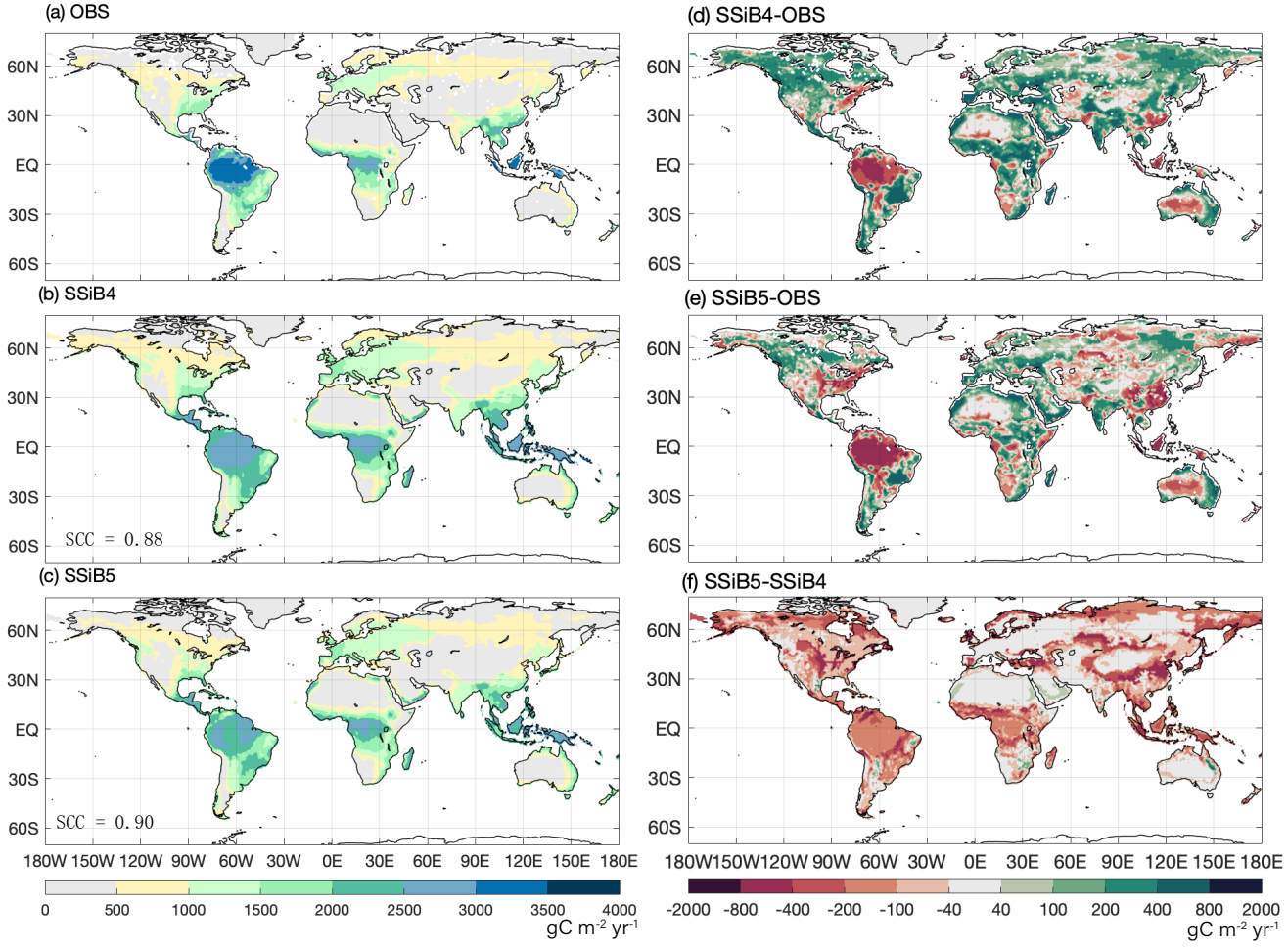

Figure 8. The 1982-2007 average gross primary production comparison for (a) FLUXNET-MTE GPP (OBS), (b) SSiB4/TRIFFID (SSiB4), and (c) SSiB5/TRIFFID/DayCent/SOM (SSiB5), and difference between (d) SSiB4-OBS, and (e) SSiB5-OBS, (f) SSiB5-SSiB4.
Note: SCC indicates the spatial correlation coefficient between model simulation and satellite-derived datasets (OBS).

https://doi.org/10.5194/egusphere-2022-1111
Preprint. Discussion started: 7 November 2022

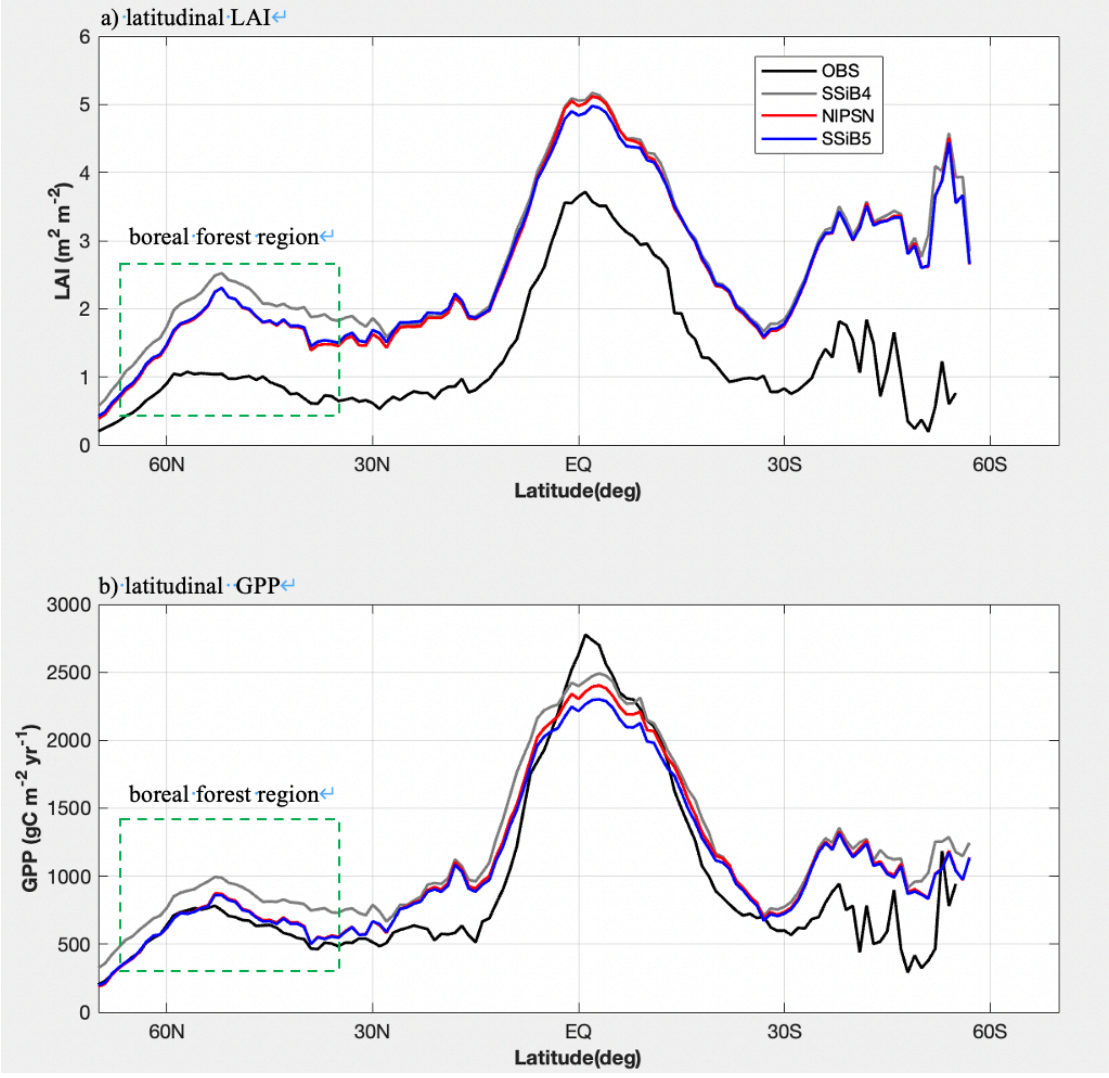

Figure 9. Intercomparisons of latitudinal LAI and GPP among OBS, SSiB4 (control), NlPSN (N limitation on photosynthesis only), and SSiB5 (all N processes) over the period 1982-2007.

https://doi.org/10.5194/egusphere-2022-1111
Preprint. Discussion started: 7 November 2022

Table 5. Regional and Global GPP for (a) FLUXNET-MTE GPP (observation), (b) SSiB4 (control), (c) NlPSN (N limitation on photosynthesis only) and (d) SSiB5 (N limitation on photosynthesis, autotrophic respiration, and phenology).

Regions	Sub-regions	GPP Mean (gC m^{-2} yr^{-1})							
		MTE		SSiB4		NlPSN		SSiB5	
		mean	bias	mean	bias	mean	bias	mean	bias
Arid and Semi-Arid Areas	West Africa	893		1147	254(28.5%)	963	70(7.9%)	915	22(2.5%)
	West NA	438		549	111(25.4%)	454	16(3.5%)	431	-7(-1.6%)
	SA Savanna	1665		1860	195(11.7%)	1763	98(5.9%)	1675	10(0.6%)
	East Africa	1228		1533	306(24.9%)	1427	199(16.2%)	1356	128(10.4%)
	East Asian semi-arid	1440		1470	30(2.1%)	1199	-241(-16.7%)	1139	-301(-20.9%)
NH High-Mid Latitude Areas	NA High-Mid Latitude	552		814	262(47.6%)	700	149(27.0%)	665	114(20.6%)
	Eurasian High-Mid	844		966	122(14.5%)	871	27(3.2%)	827	16(-2.0%)
Equator	Amazon Basin	2993		2668	-326(-10.9%)	2631	-362(-12.1%)	2500	-494(-16.5%)
	Southeast Asia	2778		2540	-238(-8.6%)	2419	-359(-12.9%)	2298	-480(-17.3%)
	Equator Africa	2522		2645	123(4.9%)	2611	89(3.5%)	2481	-42(-1.7%)
Subarctic Areas and Tibet	NA Subarctic	234		364	130(55.7%)	240	6(2.4%)	228	-6(-2.7%)
	Eurasian Subarctic	331		484	153(46.2%)	328	-3(-1.0%)	311	-20(-6.0%)
	Tibet	409		561	153(37.3%)	298	-111(-27.2%)	283	126(-30.8%)
Global		**863**		**1082**	**220(25.4%)**	**991**	**129(14.9%)**	**942**	**79(9.1%)**

Note: the numbers in parentheses are relative biases: (bias/MTE mean) x 100%

The correlation coefficients between observed and simulated monthly/annual mean GPPs are increased from 0.46/0.98 (Exp. SSiB4) to 0.50/0.99 (Exp. SSiB5), respectively (Fig. 10 and Fig. 11), showing improvement of seasonal cycle simulation in SSiB5. The correlation for the interannual variability in SSiB4 is already very high (0.98). SSiB5 shows no substantial improvement. The GPP bias in tropical Africa and boreal regions is reduced, which shows an improvement in spatial simulation (the spatial correlation coefficient increases from 0.88 to 0.90, Fig. 8). Despite the general global improvement with SSiB5, the GPP simulation in the temperate East Asian mixed forest-grassland regions seems to get worse (Fig. 8). SSiB4's simulation there is close to observations and the imposed N limitation in SSiB5 increases the magnitude of the bias. This issue needs to be further investigated in regions where the N limitation is not dominant. Further improvements, such as better ecological understanding of plant N dynamics and plant N observations, are necessary in this regional research. In addition, the negative GPP bias in the Amazon is increased (Fig. 9). This phenomenon has also appeared in the offline test in the Amazon site (the BR-Sa1 Site, Table 4). This issue will be discussed in section 5.4.

https://doi.org/10.5194/egusphere-2022-1111
Preprint. Discussion started: 7 November 2022

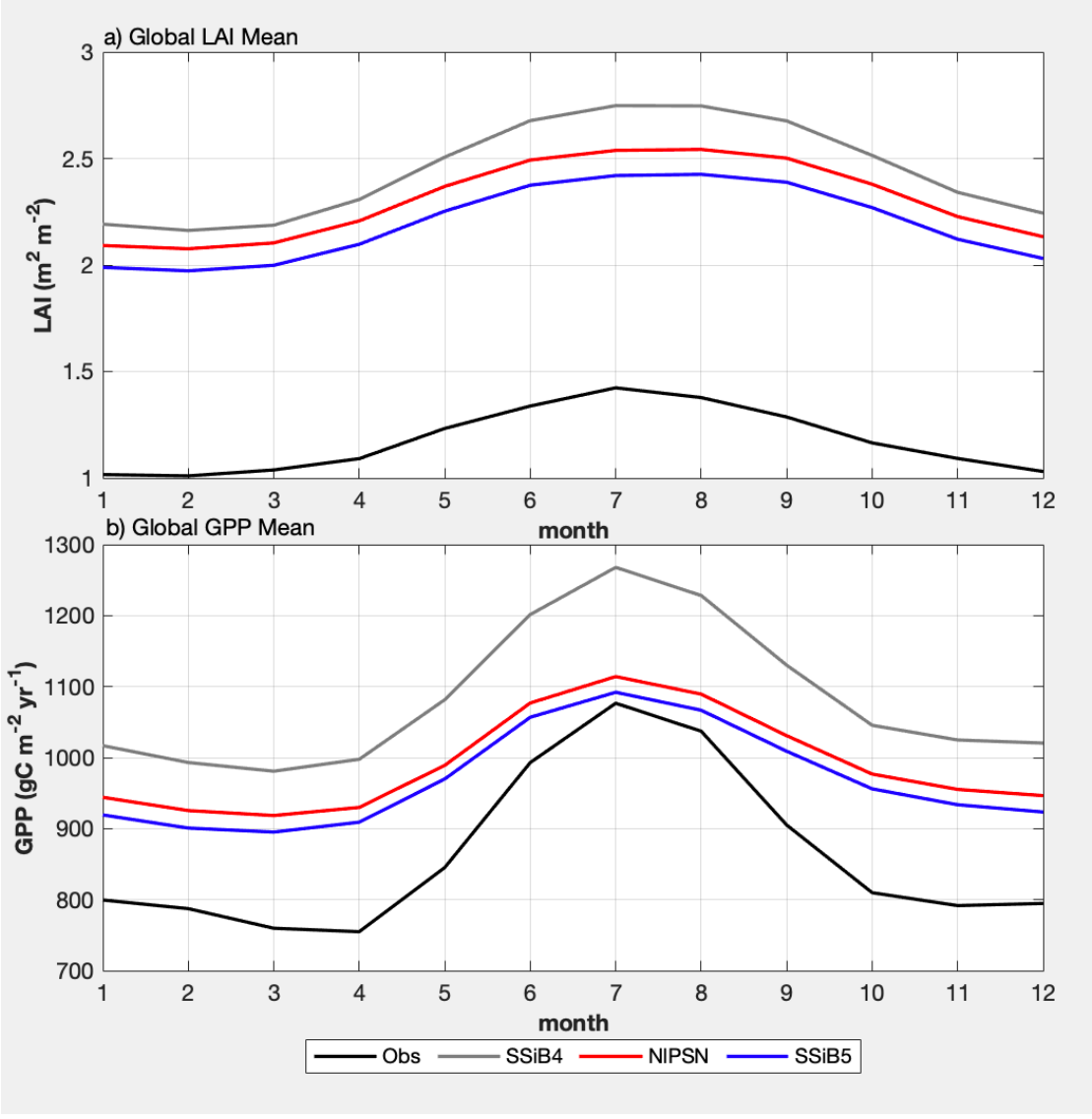

Figure 10. Same as figure 9, but for monthly LAI and GPP.

https://doi.org/10.5194/egusphere-2022-1111
Preprint. Discussion started: 7 November 2022

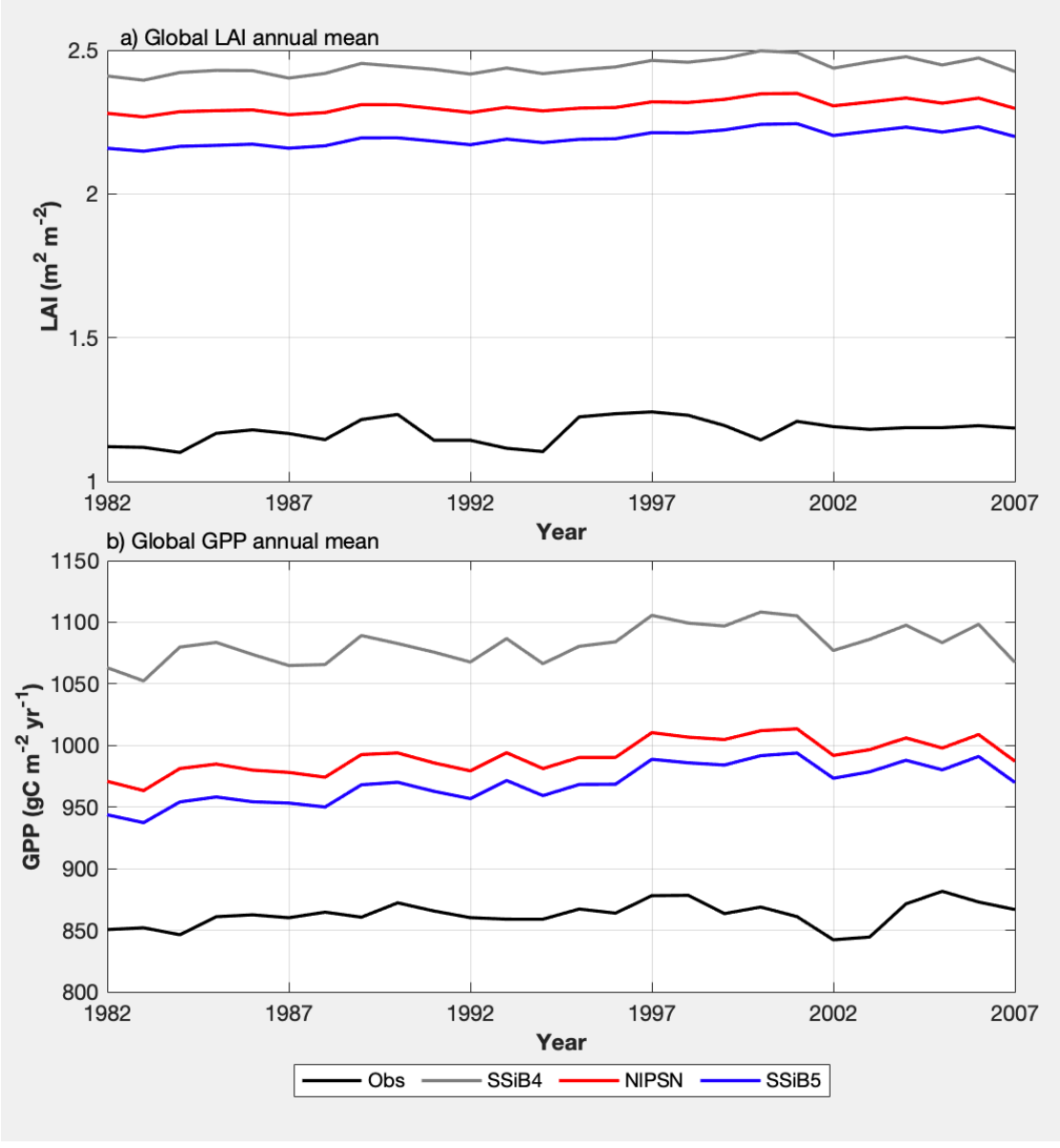

Figure 11. Same as figure 9, but for annual LAI and GPP.

Exp. SSiB5 also improved predictions of LAI compared to the control (Fig. 12). The highest LAI occurs in the tropical evergreen forest and decreases with latitude in both the observations and the model (Fig. 9). The simulated LAI in Exp. SSiB4 has a global positive bias. After introducing all nitrogen processes, the positive bias is reduced. Globally, Exp. SSiB5 has an LAI bias of 0.94/1.12 for GIMMS/GLASS, respectively (Table 6), which is lower than the LAI bias in Exp. SSiB4 (global bias = 1.26/1.44 for GIMMS/GLASS, respectively), with a 31.1% reduction in the relative bias (compared to GIMMS, Table

https://doi.org/10.5194/egusphere-2022-1111
Preprint. Discussion started: 7 November 2022

6). In addition, the correlation coefficients between observed and simulated monthly/annual average LAIs are improved from 0.49/0.97 (Exp. SSiB4) to 0.51/0.98 (Exp.SSiB5) (Fig. 10 and Fig. 11).

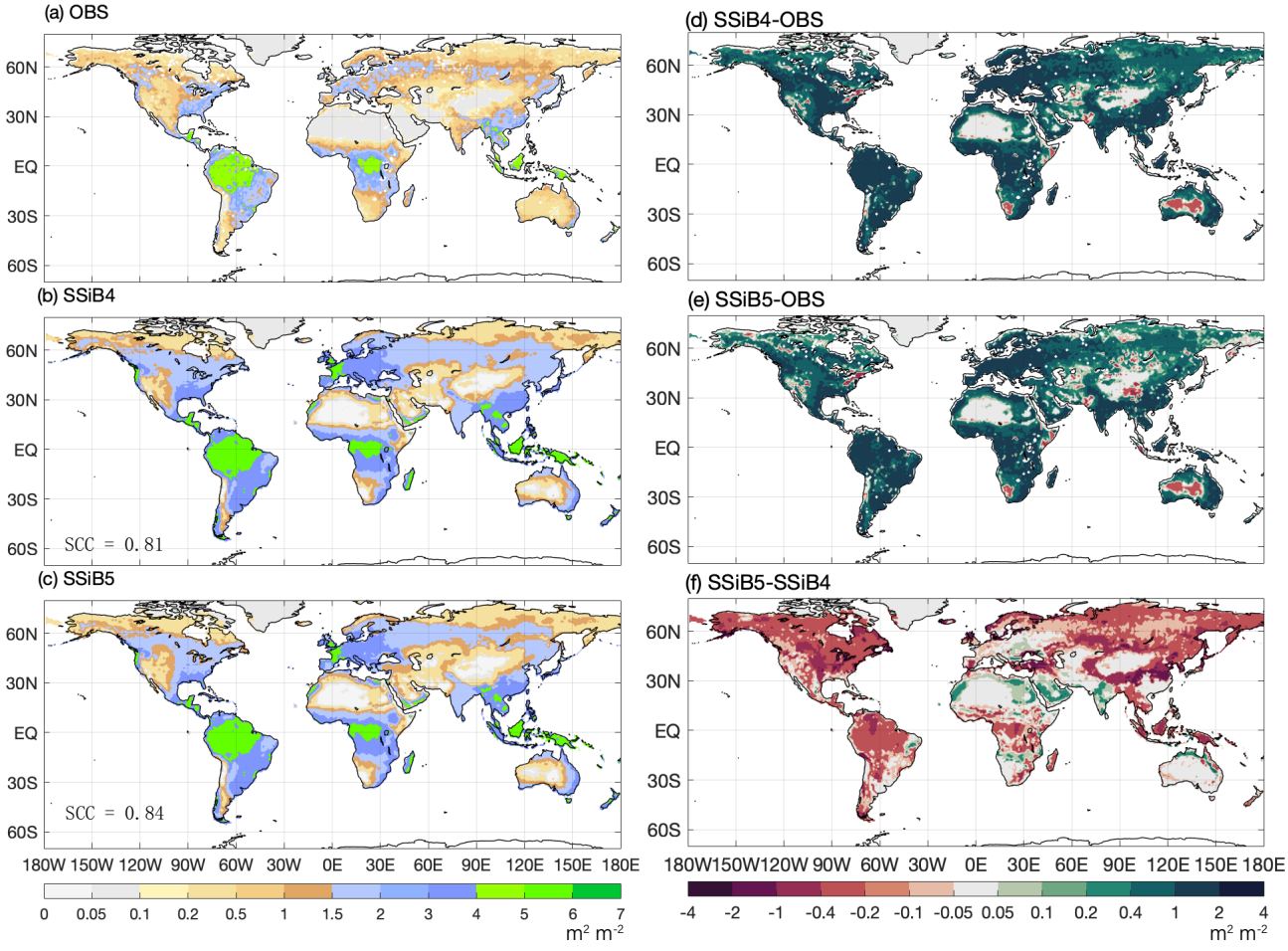

Figure 12. Same as Figure 8, but for LAI.
Note: SCC indicates the spatial correlation coefficient between model simulation and GIMMS LAI (OBS).

It is interesting to note that despite the global general LAI reduction, the SSiB5 slightly increased LAI estimates in North Africa and India (Fig. 12). The N impacts on phenology and respiration cause a slight shift in the vegetation from shrub (N. Africa) or C4 grass (India) to C3 grass in these areas. This contributes to the GPP and LAI increase (Fig. 13). In the next sections, we will further identify the effect of N limitation on each process, such as the photosynthesis process, on simulated GPP and LAI.

https://doi.org/10.5194/egusphere-2022-1111
Preprint. Discussion started: 7 November 2022

Table 6. Regional and Global LAI for (a) GIMMS LAI (observation), (b) GLASS LAI (second observation), (c) SSiB4 (control), (d) NlPSN (N limitation on photosynthesis only) and (e) SSiB5 (N limitation on photosynthesis, autotrophic respiration, and phenology). The bias is relative to GIMMS LAI.

Regions	Sub-regions	LAI Mean (m^2 m^{-2})									
		GIMMS		GLASS		SSiB4		NlPSN		SSiB5	
		mean	bias	mean	bias	mean	bias	mean	bias	mean	bias
Arid and Semi-Arid Areas	West Africa	1.08		1.01	-0.07(-6.5%)	2.04	0.96(88.9%)	1.89	0.81(75.0%)	1.73	0.65(60.2%)
	West NA	0.62		0.49	-0.13(-21.0%)	1.38	0.76(122.6%)	1.18	0.56(90.3%)	1.09	0.47(75.8%)
	SA Savanna	1.99		1.91	-0.18(-4.0%)	3.34	1.35(67.8%)	3.23	1.24(62.3%)	2.97	0.98(49.2%)
	East Africa	1.59		1.55	-0.04(-2.5%)	3.02	1.43(89.9%)	2.89	1.30(81.8%)	2.66	1.07(67.3%)
	East Asian semi-arid	1.60		1.36	-0.24(-15.0%)	3.35	1.75(109.4%)	2.84	1.24(77.5%)	2.61	1.01(63.1%)
NH High-Mid Latitude Areas	NA High-Mid Latitude	0.84		0.49	-0.35(-41.7%)	1.91	1.07(127.4%)	1.66	0.82(97.6%)	1.53	0.69(82.1%)
	Eurasian High-Mid	1.14		0.57	-0.57(-50.0%)	2.29	1.15(100.9%)	2.08	0.94(82.5%)	1.91	0.77(67.5%)
Equator	Amazon Basin	4.19		4.08	-0.11(-2.6%)	6.01	1.82(43.4%)	5.98	1.79(42.7%)	5.50	1.31(31.3%)
	Southeast Asia	3.93		3.88	-0.05(-1.3%)	4.68	0.75(19.1%)	4.68	0.75(19.1%)	4.31	0.38(9.7%)
	Equator Africa	3.83		3.76	-0.07(-1.8%)	5.74	1.91(49.9%)	5.72	1.89(49.3%)	5.27	1.44(37.6%)
Subarctic Areas and Tibet	NA Subarctic	0.32		0.14	-0.18(-56.3%)	0.71	0.39(121.9%)	0.51	0.19(59.4%)	0.47	0.15(46.9%)
	Eurasian Subarctic	0.33		0.12	-0.21(-63.6%)	0.87	0.54(163.6%)	0.65	0.32(97.0%)	0.60	0.27(81.8%)
	Tibet	0.64		0.54	-0.10(-15.6%)	1.36	0.72(112.5%)	0.81	0.17(26.6%)	0.75	0.11(17.2%)
Global		**1.18**		**1.00**	**-0.18(-15.3%)**	**2.44**	**1.26(110.8%)**	**2.31**	**1.13(95.8%)**	**2.12**	**0.94(79.7%)**

Note: the numbers in parentheses are relative biases: (bias/GIMMS mean) x 100%.

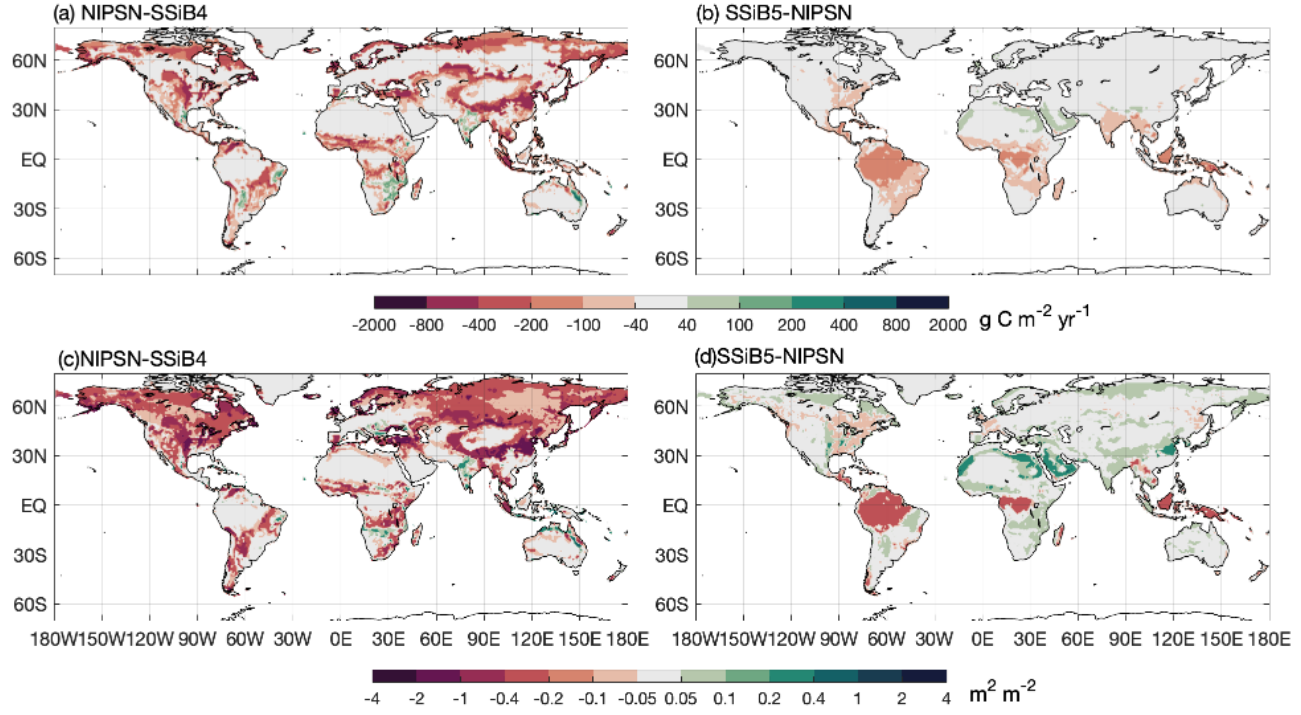

Figure 13. The 1982-2007 average gross primary production difference (a) NlPSN-SSiB4, (b) SSiB5-NlPSN, and leaf area index difference (c) NlPSN- SSiB4, (d) SSiB5- NlPSN

Note: NlPSN is N limitation on photosynthesis (Vmax) only.

https://doi.org/10.5194/egusphere-2022-1111
Preprint. Discussion started: 7 November 2022

5.3 Effects of nitrogen limitation on photosynthesis

In this section, we discuss the results from Exp. NlPSN, Exp. NlNPP, and Exp. NlGPP, which apply Eq. (7), Eq. (9a), and Eq. (9b) to scale down the $V_{c,max}$, NPP, and GPP, respectively. The highest GPP occurs in the tropical evergreen forest and decreases with increase in latitudes, which are well simulated in all three model experiments (Exp. NlPSN, Exp. NlNPP, Exp. NlGPP) (Fig. 14). However, compared to FLUXNET-MTE GPP, the simulated GPP in Exp. NlPSN has the smallest negative bias in the Amazon tropical forest and smallest positive bias in tropical Africa and boreal regions (Fig. 9 and Fig. 14). Exp. NlPSN has a lower global GPP bias (128.52 g C m^{-2} yr^{-1}) compared to FLUXNET-MTE estimates than Exp. SSiB4 does (219.50 g C m^{-2} yr^{-1}) (Fig. 14, Table 5). Exp. NlPSN has a global LAI bias of 1.13 (Fig. 15, Table 6), which is also lower than the LAI bias in Exp. SSiB4 (1.26). The largest reductions in the magnitude of the LAI bias are in the North American and Eurasian continents.

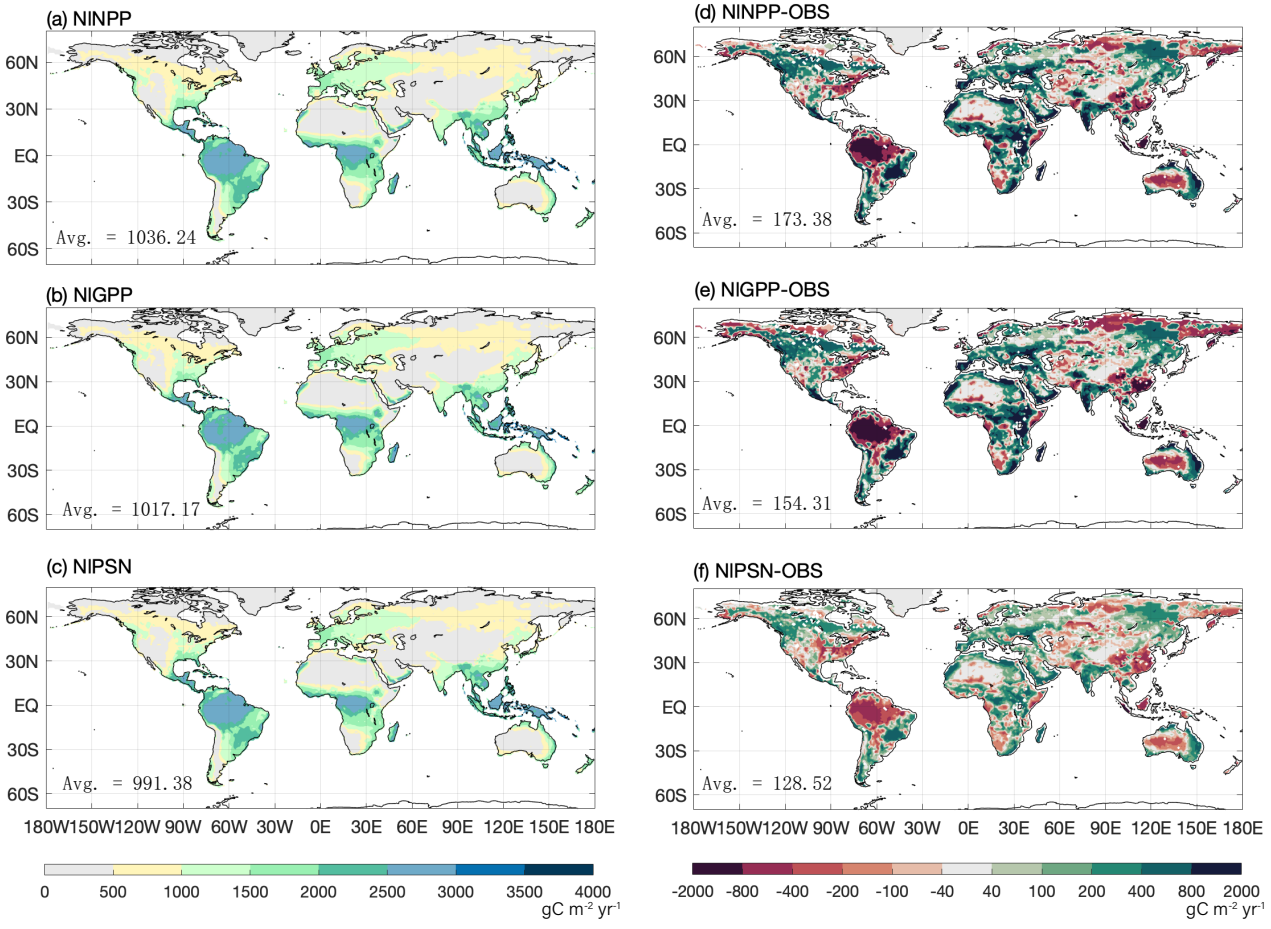

Figure 14. The 1982-2007 average gross primary production comparison for (a) NlNPP, (b) NlGPP and (c) NlPSN, (d) NlNPP- OBS, (e) NlGPP- OBS and (f) NlPSN- OBS.

https://doi.org/10.5194/egusphere-2022-1111
Preprint. Discussion started: 7 November 2022

Notes: (1) NlPSN is N limitation on photosynthesis (Vmax) only; NlNPP is N limitation on NPP only; and NlGPP is N limitation on GPP only. (2). OBS is FLUXNET-MTE GPP (OBS). (3). Avg. indicates the global average.

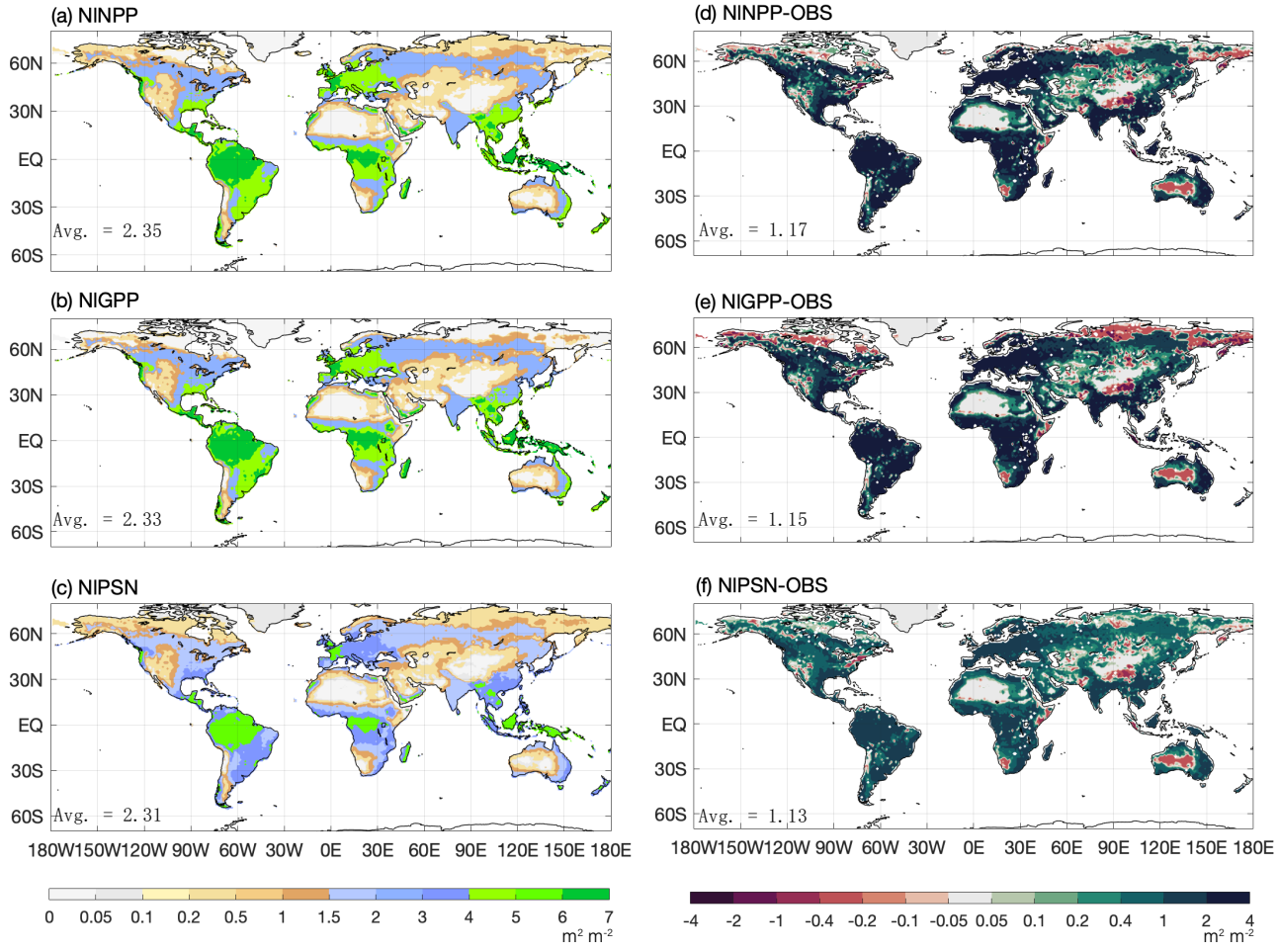

Figure 15. Same as Figure 14, but for LAI.

Among NlPSN, NlNPP, and NlGPP, Exp. NlPSN had lower global GPP bias (128.52 g C m^{-2} yr^{-1}, Fig. 14) than Exp. NlNPP (173.38 g C m^{-2} yr^{-1}) and Exp. NlGPP (154.31 g C m^{-2} yr^{-1}). Moreover, for global LAI, Exp. NlPSN's bias (1.13) is also lower than the LAI bias of Exp. NlNPP (1.17) and Exp. NlGPP (1.15). Regarding the spatial correlation, the three experiments produce about the same correlation coefficients for GPP (about 0.90, Table 7) and LAI (about 0.83, Table 7). By and large, the Exp. NIPSN approach yields better results among these three sensitivity experiments. This is because adjusting $V_{c,max}$ is the most direct and process-based one on physiology, and the most suitable for SSiB5's model structure. As a matter of fact, the results in Tables 5 and 6 show that even introducing N limitation on photosynthesis alone, Exp. NlPSN has already produced better GPP and LAI simulation compared to Exp. SSiB4, which has no N-processes.

https://doi.org/10.5194/egusphere-2022-1111
Preprint. Discussion started: 7 November 2022

Table 7. The spatial correlation coefficient (SCC) between model simulations and OBS.

LAI SCC	NlPSN	NlNPP	NlGPP
OBS	0.8370**	0.8340**	0.8246**
GPP SCC	NlPSN	NlNPP	NlGPP
OBS	0.9020**	0.8998**	0.8900**

Note: ** indicates correlation is significant at $p < 0.01$.

Furthermore, after introducing N impacts on respiration and phenology, Exp. SSiB5 further reduces GPP and LAI compared to that produced by Exp. NlPSN. Since Exp. SSiB4 and Exp. NlPSN overestimate LAI in all areas, N limitation helps Exp. SSiB5 to produce the best LAI results everywhere. However, Exp. SSiB4 and Exp. NlPSN do not overestimate GPP everywhere. The introduced N limitation does not guarantee Exp. SSiB5 produces the best GPP results in every region. For example, Exp. NIPSN already had a negative bias in the temperate East Asian mixed forest-grassland area; Exp. SSiB5 produced even greater negative bias there.

5.4 Attribution of N processes on C cycle

Despite the fact that N processes generally reduced the global GPP/LAI in our results, N limitation on photosynthesis (indicated by Exp. NlPSN – Exp. SSiB4) and on the other two N processes (N impacts on phenology and respiration, indicated by Exp. SSiB5 – Exp. NlPSN) show different regional attributions (Fig. 13, Table 5 and Table 6); i.e., in some regions, imposing the N-limitation in Exp. SSiB5 increases the bias as discussed in Section 5.2. Studies have suggested that not only N but also P limitation in some regions play a significant role in constraining the magnitude of terrestrial C uptake in response to elevated carbon dioxide and climate change (Du et al., 2020). Efforts have been made to identify regions constrained by global nutrient limitation. Some studies (Lauenroth et al., 1978; Owensby et al., 1970) show that N is a dominant limiting factor to grassland plant production in temperate systems. With N fertilizer additions, products could increases by 50% for dry grasslands and 100% for wet grasslands. Du et al. (2020) examined global N and P limitation using the ratio of site-averaged leaf N and P resorption efficiencies of the dominant species across 171 sites and found a strong latitudinal pattern of N and P limitation. N limitation prevails in boreal forests, tundra, temperate coniferous forests, and montane grasslands and shrublands, whereas phosphorus (P) has more effect in Mediterranean biomes, as well as tropical grasslands, savannas, shrublands and forests.

The LAI and GPP bias reduction between Exp. SSiB4 and Exp. SSiB5 (Fig. 8f, Fig. 12f), as well as the experiments that examine the impact of N limitation on different processes in fact provide a global N limitation pattern. Our simulations show a strong latitudinal pattern of N limitation and relatively close agreement with Du et al. (2020)'s results but provide more comprehensive information. N limitation on photosynthesis, which is shown in the difference between Exp. SSiB4 and Exp.

https://doi.org/10.5194/egusphere-2022-1111
Preprint. Discussion started: 7 November 2022

NlPSN, results in a dominant decrease in tropical Africa and boreal regions (Fig. 13a), but N impacts on phenology and respiration dominate the decline in GPP in tropical forests (Fig. 13b).

Moreover, there is a transition to N limitation at higher elevations in some lower-latitude regions (i.e., the Tibetan Plateau) (Du et al., 2020). This pattern is also captured in this study (Fig.13a, Fig. 13c). Using bias reduction of GPP/LAI to show N limitation patterns may not be sensitive to leaf N and P resorption efficiencies; however, it provides information on spatial heterogeneity and is a tool for comparing nutrient limitation globally to existing assessments based on site nutrient fertilization experiments. Plant production in the Amazon area and Australia are typically P-limited, which may explain why SSiB5's N limitation is not very effective in these areas (Fig.13a, Fig. 13c). In the future we will need to add plant-soil P processes to consider both P and N limitation.

6 Discussion and Conclusions

This study presents improvements in modelling C cycle by introducing plant N processes into the SSiB5/TRIFFID/DayCent-SOM, using DayCent-SOM to calculate the amount of N available to plants and plant soil N uptake. The approach presented in this study can also be applied to other models with similar physical and biological principles. The new C-N coupling framework allows us to use dynamic C/N ratios to represent plant resistance and self-adjustment. Since these processes can increase nutrient use efficiency and reduce the impact of N limitation through N remobilization and resorption, Vmax is no longer in linear relation with leaf N content. This is a unique advantage of our model. That said, with the new model structure, N impacts on GPP are predicted directly but not linearly with leaf N content, which is affected by the state of plant growth, autotrophic respiration, and plant phenology. By comparing site-level results SSiB4 and SSiB5 to FLUXNET GPP and surface heat fluxes from twelve sites with representative biome types and climates zones, we gained confidence in the ability of the new N processes to enhance model performance.

We systematically evaluated the model against multiple reference data sets for GPP, LAI, and global N limitation patterns. In general, with the new plant C-N coupling framework, SSiB5/TRIFFID/DayCent-SOM has a smaller absolute bias for GPP and LAI than the baseline version of SSiB4/TRIFFID (without N-processes). The main improvements are found in tropical Africa and the boreal forest, accompanied by a global decrease of the bias in GPP and LAI by 16.3% and 27.1%, respectively. The more realistic representation of dynamic C/N ratios and plant C-N framework leads to general improvements in SSiB5/TRIFFID/DayCent-SOM's global C cycling predictions. From the perspective of plant physiology, the downregulation of the canopy photosynthetic rate based on the available mineral N for growth of plant tissues is more reasonable than the simple and direct downregulation of GPP or NPP. This coupled model can better reproduce observed state variables and their emergent properties (such as GPP, NPP, LAI, and respiration). The model with the C-N coupling framework can also predict a global pattern of terrestrial N limitation.

Despite the general improvement globally, the GPP simulation in the temperate East Asian mixed forest-grassland regions seems to get worse with SSiB5 compared to SSiB4. In some regions with lower GPP than observations in SSiB4, the imposed

https://doi.org/10.5194/egusphere-2022-1111
Preprint. Discussion started: 7 November 2022

N limitation in SSiB5 would further increase the bias in the regions. This mismatch is a common issue reported in a number of publications that needs to be further investigated (Anav et al., 2015; Liu et al., 2019; Piao et al., 2013). Recently, the important influence of phosphorus availability on the terrestrial ecosystem carbon uptake has been increasingly realized. The recently initiated ecosystem-scale manipulation experiments in phosphorus-poor environments (Fleischer et al., 2019) call for the need for new phosphorus enabled LSMs to keep track of these actions (Goll et al., 2017; Reed et al., 2015). This may also explain why SSiB5's N limitation is not very effective in the tropics (Fig.13a, Fig. 13c). We plan to incorporate other plant processes, such as plant/soil phosphorus processes, to improve performance of the model in the future.

Data availability. The evaluation/reference data sets from model data discussed in this paper are archived at https://doi.org/10.5281/zenodo.7196869

Code availability. The source code of biophysical-ecosystem-biogeochemical model, SSiB version5/TRIFFID/DayCent-SOM is archived at https://doi.org/10.5281/zenodo.7297108

Author contributions. ZX, YX, MH, and YL designed the coupling strategy between SSiB4/TRIFFID and DayCent-SOM. ZX conducted the simulation with suggestions from YX, WG, and WP. ZX, YX, and MH drafted the text and ZX made the figures. All authors (ZX, YX, WG, MH, YL, and WP) have contributed to the analysis and the text.

C*ompeting interests.* The authors declare that they have no conflict of interest.

Acknowledgments This study is joint supported by the National Science Foundation, Division of Atmospheric and Geospace Sciences (Grant No. AGS-1419526, AGS-1849654), and the Fundamental Research Funds for the Central Universities (Grant No. 14380172). The authors acknowledge the use of the Cheyenne supercomputer (https://doi.org/10.5065/D6RX99HX, Computational and Information Systems Laboratory, 2019), provided by NCAR CISL, for providing HPC resources.

https://doi.org/10.5194/egusphere-2022-1111
Preprint. Discussion started: 7 November 2022

References

Aber, J. D., Goodale, C. L., Ollinger, S. V., Smith, M.-L., Magill, A. H., Martin, M. E., Hallett, R. A. and Stoddard, J. L.: Is nitrogen deposition altering the nitrogen status of northeastern forests?, Bioscience, 53(4), 375–389, doi:10.1641/0006-3568(2003)053[0375:INDATN]2.0.CO;2, 2003.

Aerts, R.: Nutrient Resorption from Senescing Leaves of Perennials: Are there General Patterns?, J. Ecol., 84(4), 597, doi:10.2307/2261481, 1996.

Aerts, R. and Berendse, F.: The effect of increased nutrient availability on vegetation dynamics in wet heathlands, Vegetatio, 76(1–2), 63–69, doi:10.1007/BF00047389, 1988.

Ali, A. A., Xu, C., Rogers, A., McDowell, N. G., Medlyn, B. E., Fisher, R. A., Wullschleger, S. D., Reich, P. B., Vrugt, J. A., Bauerle, W. L., Santiago, L. S. and Wilson, C. J.: Global-scale environmental control of plant photosynthetic capacity, Ecol. Appl., 25(8), 2349–2365, doi:10.1890/14-2111.1, 2015.Anav, A., Friedlingstein, P., Beer, C., Ciais, P., Harper, A., Jones, C., Murray-Tortarolo, G., Papale, D., Parazoo, N. C., Peylin, P., Wiltshire, A. and Zhao, M.: Spatiotemporal patterns of terrestrial gross primary production: A review, Rev. Geophys., 53(3), 785–818, doi:10.1002/2015RG000483, 2015.

Arora, V. K., Katavouta, A., Williams, R. G., Jones, C. D., Brovkin, V., Friedlingstein, P., Schwinger, J., Bopp, L., Boucher, O., Cadule, P. and Chamberlain, M. A.: Carbon – concentration and carbon – climate feedbacks in CMIP6 models and their comparison to CMIP5 models, , 4173–4222, 2020.

Beer, C., Reichstein, M., Tomelleri, E., Ciais, P., Jung, M., Carvalhais, N., Rodenbeck, C., Arain, M. A., Baldocchi, D., Bonan, G. B., Bondeau, A., Cescatti, A., Lasslop, G., Lindroth, A., Lomas, M., Luyssaert, S., Margolis, H., Oleson, K. W., Roupsard, O., Veenendaal, E., Viovy, N., Williams, C., Woodward, F. I. and Papale, D.: Terrestrial Gross Carbon Dioxide Uptake: Global Distribution and Covariation with Climate, Science (80-.)., 329(5993), 834–838, doi:10.1126/science.1184984, 2010.

Best, M. J., Pryor, M., Clark, D. B., Rooney, G. G., Essery, R. . L. H., Ménard, C. B., Edwards, J. M., Hendry, M. A., Porson, A., Gedney, N., Mercado, L. M., Sitch, S., Blyth, E., Boucher, O., Cox, P. M., Grimmond, C. S. B. and Harding, R. J.: The Joint UK Land Environment Simulator (JULES), model description – Part 1: Energy and water fluxes, Geosci. Model Dev., 4(3), 677–699, doi:10.5194/gmd-4-677-2011, 2011.

Bonan, G. B.: Forests and Climate Change : Climate Benefits of Forests, Science (80-.)., 320(June), 1444–1449, 2008.

Bonan, G. B., Hartman, M. D., Parton, W. J. and Wieder, W. R.: Evaluating litter decomposition in earth system models with long-term litterbag experiments: An example using the Community Land Model version 4 (CLM4), Glob. Chang. Biol., 19(3), 957–974, doi:10.1111/gcb.12031, 2013.

Clark, D. B., Mercado, L. M., Sitch, S., Jones, C. D., Gedney, N., Best, M. J., Pryor, M., Rooney, G. G., Essery, R. L. H., Blyth, E., Boucher, O., Harding, R. J., Huntingford, C. and Cox, P. M.: The Joint UK Land Environment Simulator (JULES), model description – Part 2: Carbon fluxes and vegetation dynamics, Geosci. Model Dev., 4(3), 701–722, doi:10.5194/gmd-4-701-2011, 2011.

https://doi.org/10.5194/egusphere-2022-1111
Preprint. Discussion started: 7 November 2022

Clarkson, D. T. and Hanson, J. B.: The Mineral Nutrition of Higher Plants, Annu. Rev. Plant Physiol., 31(1), 239–298, doi:10.1146/annurev.pp.31.060180.001323, 1980.

Collatz, G. J., Ball, J. T., Grivet, C. and Berry, J. A.: Physiological and environmental regulation of stomatal conductance, photosynthesis and transpiration: a model that includes a laminar boundary layer, Agric. For. Meteorol., 54(2–4), 107–136, doi:10.1016/0168-1923(91)90002-8, 1991.

Cox, P. M.: Description of the "TRIFFID" Dynamic Global Vegetation Model, Hadley Cent. Tech. Note-24, 2001.

Dan, L., Yang, X., Yang, F., Peng, J., Li, Y., Gao, D., Ji, J. and Huang, M.: Integration of nitrogen dynamics into the land surface model AVIM. Part 2: baseline data and variation of carbon and nitrogen fluxes in China, Atmos. Ocean. Sci. Lett., 13(6), doi:10.1080/16742834.2020.1819145, 2020.

Davies-Barnard, T., Meyerholt, J., Zaehle, S., Friedlingstein, P., Brovkin, V., Fan, Y., Fisher, R. A., Jones, C. D., Lee, H., Peano, D., Smith, B., Wärlind, D. and Wiltshire, A. J.: Nitrogen cycling in CMIP6 land surface models: Progress and limitations, Biogeosciences, 17(20), 5129–5148, doi:10.5194/bg-17-5129-2020, 2020.

Del Grosso, S. J., Parton, W. J., Mosier, A. R., Ojima, D. S., Kulmala, A. E. and Phongpan, S.: General model for N 2 O and N 2 gas emissions from soils due to dentrification, Global Biogeochem. Cycles, 14(4), 1045–1060, doi:10.1029/1999GB001225, 2000.

Del Grosso, S. J., Parton, W. J., Mosier, A. R., Holland, E. A., Pendall, E., Schimel, D. S. and Ojima, D. S.: Modeling soil CO2 emissions from ecosystems, Biogeochemistry, 73(1), 71–91, doi:10.1007/s10533-004-0898-z, 2005.

Dorman, J. L. and Sellers, P. J.: A global climatology of albedo, roughness length and stomatal resistance for atmospheric general circulation models as represented by the Simple Biosphere Model (SiB), J. Appl. Meteorol., 28(9), 833–855, doi:10.1175/1520-0450(1989)028<0833:AGCOAR>2.0.CO;2, 1989.

Drewniak, B. and Gonzalez-Meler, M.: Earth System Model Needs for Including the Interactive Representation of Nitrogen Deposition and Drought Effects on Forested Ecosystems, Forests, 8(8), 267, doi:10.3390/f8080267, 2017.

Du, E., Terrer, C., Pellegrini, A. F. A., Ahlström, A., van Lissa, C. J., Zhao, X., Xia, N., Wu, X. and Jackson, R. B.: Global patterns of terrestrial nitrogen and phosphorus limitation, Nat. Geosci., 13(3), 221–226, doi:10.1038/s41561-019-0530-4, 2020.

Evans, J. R.: Photosynthesis and nitrogen relationships in leaves of C<inf>3</inf> plants, Oecologia, 78(1), 9–19, doi:10.1007/BF00377192, 1989.

Eyring, V., Bony, S., Meehl, G. A., Senior, C. A., Stevens, B., Stouffer, R. J. and Taylor, K. E.: Overview of the Coupled Model Intercomparison Project Phase 6 (CMIP6) experimental design and organization, Geosci. Model Dev., 9(5), 1937–1958, doi:10.5194/gmd-9-1937-2016, 2016.

Farquhar, G. D., von Caemmerer, S. and Berry, J. A.: A biochemical model of photosynthetic CO2 assimilation in leaves of C3 species, Planta, 149(1), 78–90, doi:10.1007/BF00386231, 1980.

https://doi.org/10.5194/egusphere-2022-1111
Preprint. Discussion started: 7 November 2022

Fisher, J. B., Sitch, S., Malhi, Y., Fisher, R. A., Huntingford, C. and Tan, S.-Y.: Carbon cost of plant nitrogen acquisition: A mechanistic, globally applicable model of plant nitrogen uptake, retranslocation, and fixation, Global Biogeochem. Cycles, 24(1), n/a-n/a, doi:10.1029/2009gb003621, 2010.

Fleischer, K., Rammig, A., De Kauwe, M. G., Walker, A. P., Domingues, T. F., Fuchslueger, L., Garcia, S., Goll, D. S., Grandis, A., Jiang, M., Haverd, V., Hofhansl, F., Holm, J. A., Kruijt, B., Leung, F., Medlyn, B. E., Mercado, L. M., Norby, R. J., Pak, B., von Randow, C., Quesada, C. A., Schaap, K. J., Valverde-Barrantes, O. J., Wang, Y. P., Yang, X., Zaehle, S., Zhu, Q. and Lapola, D. M.: Amazon forest response to CO2 fertilization dependent on plant phosphorus acquisition, Nat. Geosci., 12(9), doi:10.1038/s41561-019-0404-9, 2019.

Foley, J. A., Levis, S., Prentice, I. C., Pollard, D. and Thompson, S. L.: Coupling dynamic models of climate and vegetation, Glob. Chang. Biol., 4(5), 561–579, doi:10.1046/j.1365-2486.1998.t01-1-00168.x, 1998.

Friedlingstein, P., Cox, P., Betts, R., Bopp, L., von Bloh, W., Brovkin, V., Cadule, P., Doney, S., Eby, M., Fung, I., Bala, G., John, J., Jones, C., Joos, F., Kato, T., Kawamiya, M., Knorr, W., Lindsay, K., Matthews, H. D., Raddatz, T., Rayner, P., Reick, C., Roeckner, E., Schnitzler, K.-G., Schnur, R., Strassmann, K., Weaver, A. J., Yoshikawa, C. and Zeng, N.: Climate–Carbon Cycle Feedback Analysis: Results from the C 4 MIP Model Intercomparison, J. Clim., 19(14), 3337–3353, doi:10.1175/JCLI3800.1, 2006.

Gerber, S., Hedin, L. O., Oppenheimer, M., Pacala, S. W. and Shevliakova, E.: Nitrogen cycling and feedbacks in a global dynamic land model, Global Biogeochem. Cycles, 24(1), 1–15, doi:10.1029/2008GB003336, 2010.

Ghimire, B., Riley, W. J., Koven, C. D., Mu, M. and Randerson, J. T.: Representing leaf and root physiological traits in CLM improves global carbon and nitrogen cycling predictions, J. Adv. Model. Earth Syst., 8(2), 598–613, doi:10.1002/2015MS000538, 2016.

Goll, D. S., Winkler, A. J., Raddatz, T., Dong, N., Colin Prentice, I., Ciais, P. and Brovkin, V.: Carbon-nitrogen interactions in idealized simulations with JSBACH (version 3.10), Geosci. Model Dev., 10(5), 2009–2030, doi:10.5194/gmd-10-2009-2017, 2017.

Gregory, J. M., Jones, C. D., Cadule, P. and Friedlingstein, P.: Quantifying carbon cycle feedbacks, J. Clim., 22(19), 5232–5250, doi:10.1175/2009JCLI2949.1, 2009.

Grosso, S. J. Del, Parton, W. J., Mosier, A. R., Ojima, D. S., Potter, C. S., Borken, W., Brumme, R., Butterbach-Bahl, K., Crill, P. M., Dobbie, K. and Smith, K. A.: General CH 4 oxidation model and comparisons of CH 4 Oxidation in natural and managed systems, Global Biogeochem. Cycles, 14(4), 999–1019, doi:10.1029/1999GB001226, 2000.

Harper, A. B., Cox, P. M., Friedlingstein, P., Wiltshire, A. J., Jones, C. D., Sitch, S., Mercado, L. M., Groenendijk, M., Robertson, E., Kattge, J., Soudzilovskaia, N. A. and Van Bodegom, P.: Improved representation of plant functional types and physiology in the Joint UK Land Environment Simulator (JULES v4.2) using plant trait information, Geosci. Model Dev., 9(7), 2415–2440, doi:10.5194/gmd-9-2415-2016, 2016.

Herbert, D. A. and Fownes, J. H.: Phosphorus limitation of forest leaf area and net primary production on a highly weathered soil, Ecosystems, 29(2), 242–25, doi:10.1007/BF02186049, 1999.

https://doi.org/10.5194/egusphere-2022-1111
Preprint. Discussion started: 7 November 2022

Hu, S., Chapin, F. S., Firestone, M. K., Field, C. B. and Chiariello, N. R.: Nitrogen limitation of microbial decomposition in a grassland under elevated CO 2, Nature, 409(6817), 188–191, doi:10.1038/35051576, 2001.

Huang, H., Xue, Y., Li, F. and Liu, Y.: Modeling long-term fire impact on ecosystem characteristics and surface energy using a process-based vegetation-fire model SSiB4/TRIFFID-Fire v1.0, Geosci. Model Dev. Discuss., 1–41, doi:10.5194/gmd-2020-122, 2020.

Hungate, B. A., Dukes, J. S., Shaw, M. R., Luo, Y. and Field, C. B.: Nitrogen and Climate Change, Science (80-.)., 302(5650), 1512–1513, doi:10.1126/science.1091390, 2003.

Jiang, L., Lu, L., Jiang, L., Qi, Y. and Yang, A.: Impact of a detailed urban parameterization on modeling the urban heat island in beijing using TEB-RAMS, Adv. Meteorol., 2014, doi:10.1155/2014/602528, 2014.

Jung, M., Reichstein, M. and Bondeau, A.: Towards global empirical upscaling of FLUXNET eddy covariance observations: Validation of a model tree ensemble approach using a biosphere model, Biogeosciences, 6(10), 2001–2013, doi:10.5194/bg-6-2001-2009, 2009.

Jung, M., Reichstein, M., Margolis, H. A., Cescatti, A., Richardson, A. D., Arain, M. A., Arneth, A., Bernhofer, C., Bonal, D., Chen, J., Gianelle, D., Gobron, N., Kiely, G., Kutsch, W., Lasslop, G., Law, B. E., Lindroth, A., Merbold, L., Montagnani, L., Moors, E. J., Papale, D., Sottocornola, M., Vaccari, F. and Williams, C.: Global patterns of land-atmosphere fluxes of carbon dioxide, latent heat, and sensible heat derived from eddy covariance, satellite, and meteorological observations, J. Geophys. Res. Biogeosciences, 116(3), doi:10.1029/2010JG001566, 2011.

Kattge, J., Knorr, W., Raddatz, T. and Wirth, C.: Quantifying photosynthetic capacity and its relationship to leaf nitrogen content for global-scale terrestrial biosphere models, Glob. Chang. Biol., 15(4), 976–991, doi:10.1111/j.1365-2486.2008.01744.x, 2009.

Kolb, K. J. and Evans, R. D.: Implications of leaf nitrogen recycling on the nitrogen isotope composition of deciduous plant tissues, New Phytol., 156(1), 57–64, doi:10.1046/j.1469-8137.2002.00490.x, 2002.

Krinner, G., Viovy, N., de Noblet-Ducoudré, N., Ogée, J., Polcher, J., Friedlingstein, P., Ciais, P., Sitch, S. and Prentice, I. C.: A dynamic global vegetation model for studies of the coupled atmosphere-biosphere system, Global Biogeochem. Cycles, 19(1), 1–33, doi:10.1029/2003GB002199, 2005.

Lauenroth, W. K., Dodd, J. L. and Sims, P. L.: The effects of water- and nitrogen-induced stresses on plant community structure in a semiarid grassland, Oecologia, 36(2), doi:10.1007/BF00349810, 1978.

LeBauer, D. S. and Treseder, K. K.: Nitrogen limitation of net primary productivity in terrestrial ecosystems is globally distributed, Ecology, 89(2), 371–379, doi:10.1890/06-2057.1, 2008.

Liu, Y., Xue, Y., Macdonald, G., Cox, P. and Zhang, Z.: Global vegetation variability and its response to elevated CO 2 , global warming, and climate variability - A study using the offline SSiB4/TRIFFID model and satellite data, Earth Syst. Dyn., 10(1), 9–29, doi:10.5194/esd-10-9-2019, 2019.

Liu Y. and Y. Xue, 2020: Expansion of the Sahara Desert and shrinking of frozen land of the Arctic. Scientific Reports. (2020) 10:4109 | https://doi.org/10.1038/s41598-020-61085-0. www.nature.com/articles/s41598-020-61085-0.

https://doi.org/10.5194/egusphere-2022-1111
Preprint. Discussion started: 7 November 2022

Ma, H.-Y., Mechoso, C. R., Xue, Y., Xiao, H., Neelin, J. D. and Ji, X.: On the connection between continental-scale land surface processes and the tropical climate in a coupled ocean-atmosphere-land system, J. Clim., 26(22), 9006–9025, doi:10.1175/JCLI-D-12-00819.1, 2013.

MacDonald, J. A., Dise, N. B., Matzner, E., Armbruster, M., Gundersen, P. and Forsius, M.: Nitrogen input together with ecosystem nitrogen enrichment predict nitrate leaching from European forests, Glob. Chang. Biol., 8(10), 1028–1033, doi:10.1046/j.1365-2486.2002.00532.x, 2002.

Makino, A. and Osmond, B.: Effects of Nitrogen Nutrition on Nitrogen Partitioning between Chloroplasts and Mitochondria in Pea and Wheat, Plant Physiol., 96(2), 355–362, doi:10.1104/pp.96.2.355, 1991.

Marmann, P., Wendler, R., Millard, P. and Heilmeier, H.: Nitrogen storage and remobilization in ash (Fraxinus excelsior) under field and laboratory conditions, Trees - Struct. Funct., 11(5), 298–305, doi:10.1007/s004680050088, 1997.

Matson, P., Lohse, K. A. and Hall, S. J.: The Globalization of Nitrogen Deposition: Consequences for Terrestrial Ecosystems, AMBIO A J. Hum. Environ., 31(2), 113–119, doi:10.1579/0044-7447-31.2.113, 2002.

May, J. D. and Killingbeck, K. T.: Effects of preventing nutrient resorption on plant fitness and foliar nutrient dynamics, Ecology, 73(5), 1868–1878, doi:10.2307/1940038, 1992.

McDowell, N., Pockman, W. T., Allen, C. D., Breshears, D. D., Cobb, N., Kolb, T., Plaut, J., Sperry, J., West, A., Williams, D. G., Williams, D. G. and Yepez, E. A.: Mechanisms of plant survival and mortality during drought: Why do some plants survive while others succumb to drought?, New Phytol., 178(4), 719–739, doi:10.1111/j.1469-8137.2008.02436.x, 2008.

Medlyn, B. E., Zaehle, S., De Kauwe, M. G., Walker, A. P., Dietze, M. C., Hanson, P. J., Hickler, T., Jain, A. K., Luo, Y., Parton, W., Oren, R. and Norby, R. J.: Using ecosystem experiments to improve vegetation models, Nat. Clim. Chang., 5(6), 528–534, doi:10.1038/nclimate2621, 2015.

Meyer-Grünefeldt, M., Calvo, L., Marcos, E., Von Oheimb, G. and Härdtle, W.: Impacts of drought and nitrogen addition on Calluna heathlands differ with plant life-history stage, J. Ecol., 103(5), 1141–1152, doi:10.1111/1365-2745.12446, 2015.

Millard, P.: Measurement of the remobilization of nitrogen for spring leaf growth of trees under field conditions, Tree Physiol., 14(7–9), 1049–1054, doi:10.1093/treephys/14.7-8-9.1049, 1994.

Morgan, J. B. and Connolly, E. L.: Plant - Soil Interactions : Nutrient Uptake, Nat. Educ. Knowl., 4(8), 2013.

Neilsen, D., Millard, P., Neilsen, G. H. and Hogue, E. J.: Sources of N for leaf growth in a high-density apple (Malus domestica) orchard irrigated with ammonium nitrate solution, Tree Physiol., 17(11), 733–739, doi:10.1093/treephys/17.11.733, 1997.

Niu, G. Y., Fang, Y. H., Chang, L. L., Jin, J., Yuan, H. and Zeng, X.: Enhancing the Noah-MP Ecosystem Response to Droughts With an Explicit Representation of Plant Water Storage Supplied by Dynamic Root Water Uptake, J. Adv. Model. Earth Syst., 12(11), doi:10.1029/2020MS002062, 2020.

Oleson, K. W., Lawrence, D. M., Bonan, G. B., Drewniak, B., Huang, M., Charles, D., Levis, S., Li, F., Riley, W. J., Zachary, M., Swenson, S. C., Thornton, P. E., Bozbiyik, A., Fisher, R., Heald, C. L., Kluzek, E., Lamarque, F., Lawrence, P. J., Leung, L. R., Muszala, S., Ricciuto, D. M. and Sacks, W.: Technical description of version 4.5 of the Community Land

https://doi.org/10.5194/egusphere-2022-1111
Preprint. Discussion started: 7 November 2022

Model (CLM), NCAR Technical Note NCAR/TN-503+STR, Natl. Cent. Atmos. Res. Boulder, CO, (July), 420pp, doi:DOI: 10.5065/D6RR1W7M, 2013.

Owensby, C. E., Hyde, R. M. and Anderson, K. L.: Effects of Clipping and Supplemental Nitrogen and Water on Loamy Upland Bluestem Range, J. Range Manag., 23(5), doi:10.2307/3896163, 1970.

Pan, Y., Liu, Y., Wentworth, G. R., Zhang, L., Zhao, Y., Li, Y., Liu, X., Du, E., Fang, Y., Xiao, H., Ma, H. and Wang, Y.: Letter to the editor: Critical assessments of the current state of scientific knowledge, terminology, and research needs concerning the ecological effects of elevated atmospheric nitrogen deposition in China, Atmos. Environ., 153, 109–116, doi:10.1016/j.atmosenv.2017.01.015, 2017.

Parton, W. J., Stewart, J. W. B. and Cole, C. V.: Dynamics of C, N, P and S in grassland soils: a model, Biogeochemistry, 5(1), 109–131, doi:10.1007/BF02180320, 1988.

Parton, W. J., Ojima, D. S., Cole, C. V. and Schimel, D. S.: A general model for soil organic matter dynamics: sensitivity to litter chemistry, texture and management, Quant. Model. soil Form. Process. Proc. Symp. Minneapolis, 1992, 1994.

Parton, W. J., Hartman, M., Ojima, D. and Schimel, D.: DAYCENT and its land surface submodel: description and testing, Glob. Planet. Change, 19(1–4), 35–48, doi:10.1016/S0921-8181(98)00040-X, 1998.

Parton, W. J., Hanson, P. J., Swanston, C., Torn, M., Trumbore, S. E., Riley, W. and Kelly, R.: ForCent model development and testing using the Enriched Background Isotope Study experiment, J. Geophys. Res. Biogeosciences, 115(4), 1–15, doi:10.1029/2009JG001193, 2010.

Pastorello, G., Trotta, C., Canfora, E., Chu, H., Christianson, D., Cheah, Y. W., Poindexter, C., Chen, J., Elbashandy, A., Humphrey, M., Isaac, P., Polidori, D., Ribeca, A., van Ingen, C., Zhang, L., Amiro, B., Ammann, C., Arain, M. A., Ardö, J., Arkebauer, T., Arndt, S. K., Arriga, N., Aubinet, M., Aurela, M., Baldocchi, D., Barr, A., Beamesderfer, E., Marchesini, L. B., Bergeron, O., Beringer, J., Bernhofer, C., Berveiller, D., Billesbach, D., Black, T. A., Blanken, P. D., Bohrer, G., Boike, J., Bolstad, P. V., Bonal, D., Bonnefond, J. M., Bowling, D. R., Bracho, R., Brodeur, J., Brümmer, C., Buchmann, N., Burban, B., Burns, S. P., Buysse, P., Cale, P., Cavagna, M., Cellier, P., Chen, S., Chini, I., Christensen, T. R., Cleverly, J., Collalti, A., Consalvo, C., Cook, B. D., Cook, D., Coursolle, C., Cremonese, E., Curtis, P. S., D'Andrea, E., da Rocha, H., Dai, X., Davis, K. J., De Cinti, B., de Grandcourt, A., De Ligne, A., De Oliveira, R. C., Delpierre, N., Desai, A. R., Di Bella, C. M., di Tommasi, P., Dolman, H., Domingo, F., Dong, G., Dore, S., Duce, P., Dufrêne, E., Dunn, A., Dušek, J., Eamus, D., Eichelmann, U., ElKhidir, H. A. M., Eugster, W., Ewenz, C. M., Ewers, B., Famulari, D., Fares, S., Feigenwinter, I., Feitz, A., Fensholt, R., Filippa, G., Fischer, M., Frank, J., Galvagno, M., Gharun, M., Gianelle, D., et al.: The FLUXNET2015 dataset and the ONEFlux processing pipeline for eddy covariance data, Sci. data, 7(1), doi:10.1038/s41597-020-0534-3, 2020.

Peñuelas, J., Poulter, B., Sardans, J., Ciais, P., Van Der Velde, M., Bopp, L., Boucher, O., Godderis, Y., Hinsinger, P., Llusia, J., Nardin, E., Vicca, S., Obersteiner, M. and Janssens, I. A.: Human-induced nitrogen-phosphorus imbalances alter natural and managed ecosystems across the globe, Nat. Commun., 4, doi:10.1038/ncomms3934, 2013.

https://doi.org/10.5194/egusphere-2022-1111
Preprint. Discussion started: 7 November 2022

Piao, S., Sitch, S., Ciais, P., Friedlingstein, P., Peylin, P., Wang, X., Ahlström, A., Anav, A., Canadell, J. G., Cong, N., Zaehle, S. and Zeng, N.: Evaluation of terrestrial carbon cycle models for their response to climate variability and to CO2 trends, Glob. Chang. Biol., 19(7), 2117–2132, doi:10.1111/gcb.12187, 2013.

Raddatz, T. J., Reick, C. H., Knorr, W., Kattge, J., Roeckner, E., Schnur, R., Schnitzler, K. G., Wetzel, P. and Jungclaus, J.: Will the tropical land biosphere dominate the climate-carbon cycle feedback during the twenty-first century?, Clim. Dyn., 29(6), 565–574, doi:10.1007/s00382-007-0247-8, 2007.

Reed, S. C., Yang, X. and Thornton, P. E.: Incorporating phosphorus cycling into global modeling efforts: A worthwhile, tractable endeavor, New Phytol., 208(2), doi:10.1111/nph.13521, 2015.

Reich, P. B., Hobbie, S. E., Lee, T., Ellsworth, D. S., West, J. B., Tilman, D., Knops, J. M. H., Naeem, S. and Trost, J.: Nitrogen limitation constrains sustainability of ecosystem response to CO2, Nature, 440(7086), 922–925, doi:10.1038/nature04486, 2006.

Reich, P. B., Tjoelker, M. G., Pregitzer, K. S., Wright, I. J., Oleksyn, J. and Machado, J. L.: Scaling of respiration to nitrogen in leaves, stems and roots of higher land plants, Ecol. Lett., 11(8), 793–801, doi:10.1111/j.1461-0248.2008.01185.x, 2008.

Richardson, A. D., Anderson, R. S., Arain, M. A., Barr, A. G., Bohrer, G., Chen, G., Chen, J. M., Ciais, P., Davis, K. J., Desai, A. R., Dietze, M. C., Dragoni, D., Garrity, S. R., Gough, C. M., Grant, R., Hollinger, D. Y., Margolis, H. A., Mccaughey, H., Migliavacca, M., Monson, R. K., Munger, J. W., Poulter, B., Raczka, B. M., Ricciuto, D. M., Sahoo, A. K., Schaefer, K., Tian, H., Vargas, R., Verbeeck, H., Xiao, J. and Xue, Y.: Terrestrial biosphere models need better representation of vegetation phenology: Results from the North American Carbon Program Site Synthesis, Glob. Chang. Biol., 18(2), doi:10.1111/j.1365-2486.2011.02562.x, 2012.

Rogers, A.: The use and misuse of V(c,max) in Earth System Models., Photosynth. Res., 119(1–2), 15–29, doi:10.1007/s11120-013-9818-1, 2014.

Sellers, P. J., Mintz, Y., Sud, Y. C. and Dalcher, A.: A Simple Biosphere Model (SIB) for Use within General Circulation Models, J. Atmos. Sci., 43(6), 505–531, doi:10.1175/1520-0469(1986)043<0505:ASBMFU>2.0.CO;2, 1986.

Selleers, P. J., S. 0. Los, C. J. Tucker, C. 0. Justice, D. A. Dazlich, G. J. Collatz, and D. A. Randall, 1996: A revised land surface param-eterization (SiB2) for atmospheric GCMs. Part II: The genera-tion of global fields of terrestrial biophysical parameters from satellite data. J. Climate, 9, 706-737.

Sheffield, J., Goteti, G. and Wood, E. F.: Development of a 50-year high-resolution global dataset of meteorological forcings for land surface modeling, J. Clim., 19(13), 3088–3111, doi:10.1175/JCLI3790.1, 2006.

Sitch, S., Smith, B., Prentice, I. C., Arneth, A., Bondeau, A., Cramer, W., Kaplan, J. O., Levis, S., Lucht, W., Sykes, M. T., Thonicke, K. and Venevsky, S.: Evaluation of ecosystem dynamics, plant geography and terrestrial carbon cycling in the LPJ dynamic global vegetation model, Glob. Chang. Biol., 9(2), 161–185, doi:10.1046/j.1365-2486.2003.00569.x, 2003.

Stenberg, J. A. and Muola, A.: How should plant resistance to herbivores be measured?, Front. Plant Sci., 8, doi:10.3389/fpls.2017.00663, 2017.

https://doi.org/10.5194/egusphere-2022-1111
Preprint. Discussion started: 7 November 2022

Talhelm, A. F., Pregitzer, K. S. and Burton, A. J.: No evidence that chronic nitrogen additions increase photosynthesis in mature sugar maple forests, Ecol. Appl., 21(7), 2413–2424, doi:10.1890/10-2076.1, 2011.

Talmy, D., Blackford, J., Hardman-Mountford, N. J., Polimene, L., Follows, M. J. and Geider, R. J.: Flexible C : N ratio enhances metabolism of large phytoplankton when resource supply is intermittent, Biogeosciences, 11(17), doi:10.5194/bg-11-4881-2014, 2014.

Thomas, R. Q., Brookshire, E. N. J. and Gerber, S.: Nitrogen limitation on land: How can it occur in Earth system models?, Glob. Chang. Biol., 21(5), 1777–1793, doi:10.1111/gcb.12813, 2015.

Thornely, J. H. M. and Johnson, I. R.: Plant Growth Modelling: A Mathematical approach to Plant and Crop Physiology, , 669, 1990.

Thornton, P. E., Lamarque, J.-F., Rosenbloom, N. A. and Mahowald, N. M.: Influence of carbon-nitrogen cycle coupling on land model response to CO<inf>2</inf> fertilization and climate variability, Global Biogeochem. Cycles, 21(4), doi:10.1029/2006GB002868, 2007.

Thum, T., Caldararu, S., Engel, J., Kern, M., Pallandt, M., Schnur, R., Yu, L. and Zaehle, S.: A new model of the coupled carbon, nitrogen, and phosphorus cycles in the terrestrial biosphere (QUINCY v1.0; revision 1996), Geosci. Model Dev., 12(11), doi:10.5194/gmd-12-4781-2019, 2019.

Vicca, S., Luyssaert, S., Peñuelas, J., Campioli, M., Chapin, F. S., Ciais, P., Heinemeyer, A., Högberg, P., Kutsch, W. L., Law, B. E., Malhi, Y., Papale, D., Piao, S. L., Reichstein, M., Schulze, E. D. and Janssens, I. A.: Fertile forests produce biomass more efficiently, Ecol. Lett., 15(6), 520–526, doi:10.1111/j.1461-0248.2012.01775.x, 2012.

Vitousek, P.: Nutrient Cycling and Nutrient Use Efficiency Author (s): Peter Vitousek Source : The American Naturalist , Vol . 119 , No . 4 (Apr ., 1982), pp . 553-572 Published by : The University of Chicago Press for The American Society of Naturalists Stable URL, , 119(4), 553–572, 1982.

Vitousek, P. and Howarth, R.: Nitrogen limitation on land and in the sea: How can it occur?, Biogeochemistry, 13(2), 3646–3653, doi:10.1007/BF00002772, 1991.

Wang, Y. P., Law, R. M. and Pak, B.: A global model of carbon, nitrogen and phosphorus cycles for the terrestrial biosphere, Biogeosciences, 7(7), 2261–2282, doi:10.5194/bg-7-2261-2010, 2010.

Xiao, Z., Liang, S., Wang, J., Chen, P., Yin, X., Zhang, L. and Song, J.: Use of general regression neural networks for generating the GLASS leaf area index product from time-series MODIS surface reflectance, IEEE Trans. Geosci. Remote Sens., 52(1), 209–223, doi:10.1109/TGRS.2013.2237780, 2014.

Xue, Y., Sellers, P. J., Kinter, J. L. and Shukla, J.: A Simplified biosphere model for global climate studies, J. Clim., 4(3), 345–364, doi:10.1175/1520-0442(1991)004<0345:ASBMFG>2.0.CO;2, 1991.

Xue, Y., Juang, H.-M. H., Li, W.-P., Prince, S., DeFries, R., Jiao, Y. and Vasic, R.: Role of land surface processes in monsoon development: East Asia and West Africa, J. Geophys. Res. D Atmos., 109(3), 2004.

https://doi.org/10.5194/egusphere-2022-1111
Preprint. Discussion started: 7 November 2022

Xue, Y., De Sales, F., Vasic, R., Mechoso, C. R., Arakawa, A. and Prince, S.: Global and seasonal assessment of interactions between climate and vegetation biophysical processes: A GCM study with different land-vegetation representations, J. Clim., 23(6), 1411–1433, doi:10.1175/2009JCLI3054.1, 2010.

Yang, X., Dan, L., Yang, F., Peng, J., Li, Y., Gao, D., Ji, J. and Huang, M.: The integration of nitrogen dynamics into a land surface model. Part 1: model description and site-scale validation, Atmos. Ocean. Sci. Lett., 12(1), doi:10.1080/16742834.2019.1548246, 2019.

Yu, L., Ahrens, B., Wutzler, T., Zaehle, S. and Schrumpf, M.: Modeling Soil Responses to Nitrogen and Phosphorus Fertilization Along a Soil Phosphorus Stock Gradient, Front. For. Glob. Chang., 3, doi:10.3389/ffgc.2020.543112, 2020.

Zaehle, S., Jones, C. D., Houlton, B., Lamarque, J. F. and Robertson, E.: Nitrogen availability reduces CMIP5 projections of twenty-first-century land carbon uptake, J. Clim., 28(6), 2494–2511, doi:10.1175/JCLI-D-13-00776.1, 2015.

Zhan, X., Xue, Y. and Collatz, G. J.: An analytical approach for estimating CO 2 and heat fluxes over the Amazonian region, Ecol. Modell., 162(1–2), 97–117, doi:10.1016/S0304-3800(02)00405-2, 2003.

Zhang, Z., Xue, Y., MacDonald, G., Cox, P. M. and Collatz, G. J.: Investigation of North American vegetation variability under recent climate: A study using the SSiB4/TRIFFID biophysical/dynamic vegetation model, J. Geophys. Res., 120(4), 1300–1321, doi:10.1002/2014JD021963, 2015.

Zhu, Q., Riley, W. J., Tang, J., Collier, N., Hoffman, F. M., Yang, X. and Bisht, G.: Representing Nitrogen, Phosphorus, and Carbon Interactions in the E3SM Land Model: Development and Global Benchmarking, J. Adv. Model. Earth Syst., 11(7), doi:10.1029/2018MS001571, 2019.

Zhu, Z., Bi, J., Pan, Y., Ganguly, S., Anav, A., Xu, L., Samanta, A., Piao, S., Nemani, R. R. and Myneni, R. B.: Global data sets of vegetation leaf area index (LAI)3g and fraction of photosynthetically active radiation (FPAR)3g derived from global inventory modeling and mapping studies (GIMMS) normalized difference vegetation index (NDVI3G) for the period 1981 to 2, Remote Sens., 5(2), 927–948, doi:10.3390/rs5020927, 2013.